Vibration and vibration-torsion levels of the S_1 state of *para*-fluorotoluene in the 580–830 cm^{-1} range: interactions and coincidences

William D. Tuttle, Adrian M. Gardner, Laura E. Whalley, and Timothy G. Wright[a]

School of Chemistry, University of Nottingham, University Park, Nottingham NG7 2RD, UK

[a] Tim.Wright@nottingham.ac.uk

Abstract

A study of the vibration and vibration-torsion levels of *para*-fluorotoluene (*p*FT) in the 580–830 cm^{-1} region is presented, where a number of features are located whose identity is complicated by interactions and overlap. We examine this region with a view to ascertaining the assignments of the bands; in particular, identifying those that arise from interactions involving various zero-order states (ZOSs) involving both vibrations and torsions. Resonance-enhanced multiphoton ionization (REMPI) is employed to identify the wavenumbers of the relevant transitions and subsequently zero-kinetic-energy (ZEKE) spectra are recorded to assign the various eigenstates. In some cases, a set of ZEKE spectra are recorded across the wavenumber range of a REMPI feature, and we construct what we term a two-dimensional ZEKE (2D-ZEKE) spectrum, which allows the changing ZOS contributions to the eigenstates to be ascertained. Assignment of the observed bands is aided by quantum chemical calculations and all b_1 and a_2 symmetry vibrational wavenumbers are now determined in the S_1 state and cation, as well as those of the D_{10} vibration. We also compare with the activity seen in the corresponding $S_1 \leftarrow S_0$ spectrum of *para*-difluorobenzene.

I. INTRODUCTION

The assignment of the vibrational structure in electronic absorption spectra is fundamental to understanding geometric and electronic structure changes that occur as the result of the excitation. This relies both on knowing the wavenumber of the vibrations as well as the atomic motion associated with them. In addition, for molecules with internal rotors, such as a methyl group, the establishing of torsion and vibration-torsion (vibtor) wavenumbers is important. Such knowledge can also be used in further resonant experiments to gain information on other electronic states and cations as well as in probing photophysical phenomena in the frequency and time domains. This picture can become more complicated as a result of vibrational and vibration-torsional interactions, and this will be discussed later in the present work.

Here, we concentrate on substituted benzenes and in particular the probing of the S_1 electronic state. This can be done via dispersed fluorescence (DF) or via a photoelectron (PE) spectroscopy (PES) technique, where the S_1 state is the resonant intermediate in each case. By recording spectra following excitation of different eigenstates, the changing activity in the DF or PE spectra can be used to unravel the various couplings. In turn, this knowledge is critical to an understanding of the stability of molecules following photoexcitation and it also opens up avenues in the control of chemical reactions using ultrashort (ps and fs) lasers. As such, an understanding of the vibrational and vibration-torsional interactions that occur in simple molecules can give insight into those that occur in larger molecules, such as biomolecules. Furthermore, studies on molecules that are related by simple changes in their structure are particularly important in being able to ascertain how such differences affect the overall behaviour of larger molecules.

In the present work, the focus of the new spectra is *para*-fluorotoluene (*p*FT), but comparison with the activity in *para*-difluorobenzene (*p*DFB) will be made. In previous work, we have shown that the activity seen in both resonance-enhanced multiphoton ionization (REMPI) and zero-kinetic-energy (ZEKE) spectroscopy was similar for *p*DFB, *p*FT and *para*-xylene (*p*Xyl), in the 0-600 cm^{-1} range.[1, 2]

In the following, we make a detailed study of a 250 cm^{-1} section of the $S_1 \leftarrow S_0$ REMPI spectrum of *p*FT from 580–830 cm^{-1} in which are located a number of features that will be shown to be composed of transitions involving a number of interacting or overlapping vibrational and vibtor levels. The assignments are made on the basis of quantum chemical calculations combined with the results of ZEKE spectra recorded across each feature. We also compare with the $S_1 \leftarrow S_0$ fluorescence study for *p*DFB,[3] and a ZEKE study[4] will also be referred to. Reference will also be made to our recent work on the 0–570 cm^{-1} region of the spectrum of

*p*FT[5] (see also upcoming work from the Lawrance group[6]). We also note that, when considering the likelihood of a vibrational or vibtor assignment, we consider whether it might arise from a coupling with an established bright transition. In particular, we note that small differences ($\leq$ 3) in vibrational quantum number between coupled levels are favoured;[7] on top of this, Δm = 0 changes in torsional quantum number between coupled states are significantly more likely than higher changes, with Δm = 3 transitions being expected weakly, and higher changes in multiples of three even weaker;[2,6,8] the likelihood of coupled vibtor levels would be a combination of these two factors.

Previous work on the $S_1 \leftarrow S_0$ transition in *p*FT has been reported by Cave and Thompson[9] who presented a wide wavenumber scan of the spectrum of the vapour, apparently at room temperature. Discussion of the spectrum was only given in terms of intervals and no specific assignment of vibrational or torsional levels was given. Cvitaš and Hollas[10] published higher-resolution spectra of the origin band and various nearby sequence bands. Seliskar et al.[11] presented a high-resolution scan of a wide range of the $S_1 \leftarrow S_0$ absorption spectrum under low-pressure ambient conditions, and also a laser-induced fluorescence (LIF) spectrum under jet-cooled conditions. They also provided suggested assignments of some of the vibrational bands in terms of Wilson[12]/Varsányi[13] labels, which are not really applicable.[14,15] Okuyama et al.[16] also presented an LIF spectrum of *p*FT in their study of the *ortho*, *meta* and *para* conformers; again, assignments were given in terms of Wilson[12]/Varsányi[13] labels. Some of the low-wavenumber bands have been reassigned to vibration-torsion (vibtor) levels by Zhao,[17] and confirmed in our recent work.[5] In earlier work from our group,[18] we had used the assignments of Okuyama et al.[16] in assigning ZEKE spectra recorded via various levels, unaware that some of the assignments of the lower-wavenumber features had been superseded by those in Zhao's thesis[17] (some of those latter reassignments are implicit in Ref. 19). In our earlier work,[18] we assigned the two levels at ~ 800 cm^{-1} to different totally-symmetric fundamentals, but one of these was reassigned to an overtone level in Ref. 20. In Ref. 21, these same two levels were assigned as a Fermi resonance (FR) pair of bands involving the same levels noted in Ref. 20.

II. EXPERIMENTAL

The apparatus has been described previously in detail elsewhere.[22,23] Briefly, the focused, frequency-doubled outputs of the two dye lasers were overlapped spatially and temporally and passed through a vacuum chamber coaxially and counterpropagating. Here they intersected a free jet expansion between two biased electrical grids located in the extraction region of a time-of-flight mass spectrometer, which was employed in the REMPI experiments. These grids were also used in the ZEKE experiments by application of

pulsed voltages, giving typical fields (*F*) of ~10 V cm^{-1}, after a delay of up to 2 μs, where this delay was minimized while avoiding the introduction of excess noise from the prompt electron signal. ZEKE bands had widths of ~5-7 cm^{-1}, even though $\sqrt{F}$ relationships would suggest the widths should be significantly greater, because of the well-known decay of the lower-lying Rydberg states accessed in the pulsed-field ionization process.[24]

The excitation laser was a dye laser (Sirah Cobra-Stretch) operating with C540A and was pumped with the third harmonic (355 nm) of a Surelite III Nd:YAG laser. The ionization laser was a dye laser (Sirah Cobra-Stretch) operating with Pyromethene 597. In each case, this laser was pumped with the second harmonic (532 nm) of a Surelite I Nd:YAG laser. The fundamental outputs produced by each dye laser were frequency doubled using BBO and KDP crystals for the pump and probe lasers, respectively.

The vapour above room temperature *para*-fluorotoluene (99% purity, Alfa Aesar) was seeded in ~1.5 bar of Ar and the gaseous mixture passed through a General Valve pulsed nozzle (750 μm, 10 Hz, opening time of 180–210 μs) to create the free jet expansion.

III. CALCULATIONAL DETAILS

In a number of cases below, some reliance is placed upon calculated vibrational wavenumbers. We have undertaken an unpublished study of the effect of basis set and level of theory for the reliability of calculating the vibrational wavenumbers of the S_1 state, our conclusions are that configuration interaction with singles (CIS) and complete-active space self-consistent field (CASSCF) methods appear to be unreliable, likely because the underlying Hartree-Fock (HF) wavefunction is unstable[25] – something that is known for benzene.[26] On the other hand, with caveats, time dependent (TD-)B3LYP calculations appear to perform much better and we report the results of those calculations here – in line with the increased stability of DFT-based methods over HF-based ones.[26] We find that basis sets are not a significant factor in the reliability or otherwise of the results, as long as the basis set is of a reasonable size; in particular, aug-cc-pVTZ basis sets are adequate. In the present work, therefore, we report results for the S_1 and D_0^+ states of *p*FT, with the results scaled by 0.97[27] to correct both for anharmonicity and other weaknesses in the method. For the cation, the UB3LYP calculations had $\langle S^2 \rangle$ values of ~0.76 and these have proven reliable in a wide range of previous work. Our strategy therefore was to identify possible assignments of the ZEKE spectra, and then use the S_1 vibrational wavenumbers to confirm the assignments or otherwise. Although occasionally caution is merited, we shall find that we are generally able to assign vibrational bands in the REMPI spectra that are

consistent with activity seen in the ZEKE spectra; thus providing some further evidence that the TD-B3LYP calculated S_1 vibrational wavenumbers are trustworthy. Table I shows the calculated values for *p*FT; in addition, the corresponding sets of values for *p*DFB are shown, which will form part of the discussion below.

Assuming the error in the calculation of the vibrational wavenumbers is similar for *p*FT and *p*DFB, then we would expect the ratio of the experimental to the theoretical value to be similar between the two molecules, and we occasionally test assignments against this criterion.

IV. RESULTS AND DISCUSSION

A. Nomenclature and Labelling

1. Vibrational Labelling

Some of the levels considered here have been used to study vibrational coupling using both fluorescence spectroscopy[28] and time-resolved PES using picosecond lasers.[21,29,30,31] We note that in those papers, a combination of Wilson[12]/Varsányi[13] and Mulliken[32]/Herzberg[33] notation was employed. As we have previously noted, Wilson notation is inappropriate because of the large change in the forms of the vibrations, from benzene to *p*FT;[15] also, the Varsányi notation is inconsistent in its treatment of different molecules (and rather confusingly also uses Wilson labels).[14,15] We also note that the use of Mulliken labels, initiated in Ref. 29 for *p*FT, is inconsistent as the list includes the CH_3-localized vibrations, yet the C_{2v} point group is used for the numbering; in any case, the Mulliken labels would be different for *p*FT and *p*DFB making comparison between these molecules difficult. We shall comment on previous assignments alongside our assignments in terms of the D_i labels from Ref. 15. (The various labels used in previous work have been included in Table I to aid the reader in referring between different studies.)

Some assignments will involve vibtor levels and for these, the G_{12} molecular symmetry group (MSG) is appropriate, and so we shall use these labels when required. In addition, torsional levels will be labelled via their *m* quantum number. The reader may find it useful to refer to our previous work[5] if they are not familiar with these labels. When referring to pure vibrational levels, we shall often simply use the C_{2v} point group labels (i.e. we treat the methyl group as a point mass on these occasions), with the correspondence between these and G_{12} symmetry labels given in Table II. Calculation of the overall symmetry of a vibrational combination band can be found from a direct product table for the C_{2v} point group. For a vibtor level, it is

necessary to use the corresponding G_{12} label for the vibration (Table II), and then find the direct product with the symmetry of the torsion, noting that a D_{3h} point group direct product table can be used, since the G_{12} MSG and the D_{3h} point group are isomorphic. The symmetries of the m levels are also given in Table II.

Under the free-jet expansion conditions employed here, the molecules are all expected to be cooled to their zero-point vibrational level and thus all $S_1 \leftarrow S_0$ pure vibrational excitations are expected to be from this level. In contrast, owing to nuclear-spin and rotational symmetry, the molecules can be in one of the m = 0 or m = 1 torsional levels.[2,5,8]

2. Vibrational Coupling

Each molecule has a set of vibrational normal modes that, within the harmonic approximation, constitute the various allowed coherent motions of the atoms that keep the centre of mass stationary with respect to a system of axes that rotates and translates with the molecule. In principle, this picture holds no matter how close the vibrations are in wavenumber, as long as we remain within the harmonic model. When comparing between similar molecules, then these normal modes might be expected to look very similar; however, it is found that the effect of changing the mass can have quite a dramatic effect on some of the vibrations. As a consequence, even within the harmonic model, the normal modes of one molecule may be quite different from those of a related one, such as between benzene and fluorobenzene,[14] and between benzene and *p*DFB.[15] There will then be the various combination and overtone levels associated with these.

If we now consider anharmonicity then, if the vibrational levels of a particular molecule are far enough apart in wavenumber, the interactions between them will be minimal. In this case, the eigenstates will correspond to these vibrations, which each will be anharmonic vibrations corresponding to a particular normal mode. The difference between the well-separated anharmonic normal modes and the harmonic normal modes can be termed “diagonal anharmonicity”. If, however, an anharmonic fundamental is close in wavenumber to one or more combination or overtone vibrations that has the same overall symmetry, then “off-diagonal” anharmonic interactions can occur. The non-interacting levels are termed zero-order states (ZOSs), and their interaction leads to the formation of eigenstates that are linear combinations of these, and will be at different wavenumbers to the original ZOSs.[33] This is most likely to occur when the ZOSs are energetically close together. For two interacting states, this is termed a Fermi resonance,[34] while for more than two levels we term this a complex Fermi resonance. For molecules that contain a hindered internal rotor, the ZOSs can also be torsional or vibtor levels and so these can also therefore become involved in the eigenstates, thus

involving further degrees of freedom. In general, these interactions lead to eigenstates that involve atomic motions that are more dispersed throughout the molecule and so the ZOS mixing promotes dispersal of energy through the molecule.

In electronic spectroscopy, if we assume a non-coupled picture initially, then a zero-order vibrational or vibtor levels can be bright (i.e. it has a significant transition intensity) or dark (i.e. it has no, or a very small transition intensity); these are often termed a zero-order bright state (ZOBS) and a zero-order dark state (ZODS), respectively. Following interaction, the resulting eigenstates will be composed of mixtures of ZOBS and ZODS character. As well as shifts in the observed positions of spectral lines from those expected, the interaction can give rise to the appearance of "extra" spectral lines. In the simplest case of one ZOBS interacting with one ZODS, then two eigenstates will be formed (corresponding to a sum and difference of the ZOBS and ZODS), both of which will appear in the electronic spectrum, by virtue of the ZOBS character. In the experiments performed here, nanosecond lasers are employed, and individual eigenstates (ignoring rotational energy levels) can usually be picked out in the spectrum. By observing projections of these eigenstates onto those in another state either by DF, or by photoionization and recording photoelectron spectra, insight into the ZOS make-up of the excited state eigenfunctions can be determined.

Later, we shall also refer to time-resolved experiments, such as those in Ref. 21, which make use of picosecond lasers, whose linewidth is ~ 15 cm^{-1}. As such, more than one eigenstate can be excited coherently, and this forms what is termed a wavepacket – i.e. a coherent superposition of more than one eigenstate. In the simplest case mentioned above, of one ZOBS interacting with one ZODS, then the two eigenstates will initially be out-of-phase and evolve in time, at time zero the wavepacket will look like the ZOBS, but then evolve to resemble the ZODS. If no loss mechanisms are present, then oscillation between these two limiting cases will continue ad infinitum – a quantum beat. Additionally, if more than two eigenstates are covered by the laser pulse then the wavepacket, and so the quantum beating pattern, may be more complicated. In such experiments, photoionization is usually the method of choice, since fluorescence lifetimes are often longer than the timescale for wavepacket evolution. Additionally, the photoionization probe can occur at variable chosen delays, giving great insight into the time-dependent dynamics. As with the nanosecond experiments, projection of the excited state eigenstates (now a wavepacket) onto those of the cation can, in principle, allow the ZOS make-up to be ascertained, particularly if the corresponding ZOSs are well-separated in the cation. It should be noted that in the picosecond experiments, the populations of the eigenstates do not change with time, unless there is some additional photophysical process occurring; the variations one sees in the time-resolved photoelectron spectra are

caused by the dephasing and rephasing of the eigenstates in the wavepacket. If such variations can be recorded over a large enough timescale, then Fourier transform can be used to obtain the energy separations between the component eigenstates.[21]

3. Transitions

When designating transitions we shall generally omit the lower level, since: in REMPI spectra it will be obvious from the jet-cooled conditions; while in ZEKE spectra the intermediate S_1 state assignment will be part of the presented discussion. Vibrational transitions will be indicated by the number, *i*, of the D_i vibration, followed by the upper state quantum number; torsional transitions will be indicated by *m* followed by the quantum numbers in the usual way. Finally, vibration-torsional transitions will be indicated by a combination of the vibrational and torsional transition terms. Mostly, band positions will be given relative to the origin transition in REMPI spectra, or relative to the adiabatic ionization in ZEKE spectra.

B. Overall Comments on the REMPI Spectrum

In Figure 1 we show an overview of the REMPI spectra (0–830 cm^{-1}) of *p*FT and *p*DFB. The *p*DFB spectrum was obtained as discussed in Ref. 5. As noted above, the 0–570 cm^{-1} (unshaded) region of the REMPI spectrum of *p*FT has been discussed and compared to that of *p*DFB and *p*Xyl in previous work.[1,5] Here, we concentrate on the higher wavenumber (shaded) section of the *p*FT spectrum. At various points we shall cross-reference to our *p*DFB REMPI spectrum[1] and comment on the assignments from the fluorescence study of Knight and Kable,[3] where appropriate.

We break the 580–830 cm^{-1} section of the REMPI spectrum down into three key regions, based upon both the energetic proximity of features and the activity seen in the ZEKE spectra. For the ease of the reader, in each case we will present a figure that will display the appropriate region of the REMPI spectrum, as well as the corresponding ZEKE spectra, and then discuss the assignments.

Assignment of a spectrum was initially carried out via the observed activity in the ZEKE spectra, since we expect the calculated vibrational wavenumbers to be more reliable for the cation. In general, the strongest band in the ZEKE spectrum is expected to correspond to $\Delta v = 0$ for a pure vibrational transition – i.e. where the vibrational quantum number(s) in the cation are the same as the intermediate S_1 level – or alternatively, the $\Delta(v,m) = 0$ transition, where both the vibrational and torsional quantum numbers in the cation are the

same as the intermediate level. On occasion, for convenience, we shall employ $\Delta v = 0$ also to imply $\Delta(v,m) = 0$ transitions. Cross-reference was then made to the calculated S_1 vibrational wavenumbers in Table I, as discussed in Section III. Particularly useful were the shifts upon ionization, with large shifts for a $\Delta v = 0$ band indicating the involvement of one or more b_1 or a_2 vibrations. We also note that we expect mainly to see vibrations of a_1 (a_1' in G_{12}) and b_2 (a_1'' in G_{12}) symmetry in the $S_1 \leftarrow S_0$ spectrum for *p*FT, with the former being Franck-Condon (FC) allowed, and the latter arising from Herzberg-Teller (HT) vibronic coupling. (It is also the case that a_1 (a_1' in G_{12}) symmetry vibrations can have their activity affected by HT coupling.)[35] We were then also able to compare the observed spectral activity to that in *p*DFB, and further compare to the assignments given by Knight and Kable.[3]

Note that in the following, and given in Table I, as well as determining a number of vibrational wavenumbers for the first time, we have also revised some of the relative wavenumbers slightly from those given in previous work. The S_1 revised values are taken from REMPI spectra recorded on different days and also using different lasers, and the close agreement between the values obtained in both cases gives confidence in these revised values. Similarly, there are some revised relative wavenumbers from the ZEKE spectra, with the present values superseding the former.

C. 580–750 cm^{-1}

This region of the REMPI spectrum shows a number of weak features as may be seen in the top trace of Figure 2, and we have indicated the excitation positions that we employed for the ZEKE spectra with labels A–I. These labels correspond to discrete bands except for positions D and F, which correspond to apparent shoulders on bands, and so might be indicative of overlapping features. We briefly discuss the assignments of these weak bands by reference to the ZEKE spectra also presented in Figure 2. To our knowledge none of these REMPI bands has been discussed in previous work. As noted in Section IV.D, it is possible to see bands arising from *p*FT-Ar complexes in this region of the spectrum; however, under the optimized conditions employed to record the REMPI spectrum in Figure 2, such bands are absent.

1. Band A

The weak Band A in the REMPI spectrum at 605.5 cm^{-1} is at the expected position for the transition to the D_{28} $m = 3(+)$ vibtor level, denoted $28^1m^{3(+)}$, which is totally symmetric (a_1') in G_{12}. The assignment of the 28^1 fundamental band was made in Ref. 18 and a discussion of the assignment of the torsional levels and low-

wavenumber vibration-torsional (vibtor) levels is given in Ref. 5. In the present work, the most intense ZEKE band is in the expected position for the D_{28} m= 3(+) level in the cation at 623 cm^{-1}. Other, very weak bands are seen in the ZEKE spectrum, with a band at 893 cm^{-1} being assignable to $19^{1}28^{1}m^{3(+)}$ – a vibronically induced band.[5] Assignments for the bands at 854 cm^{-1} and 929 cm^{-1} are less certain, with tentative, but consistent ones being $19^{1}28^{1}$ and $14^{1}28^{1}$, respectively. These transitions involve combinations of D_{28} with each of D_{14} and D_{19} – such combinations are commonly present in ZEKE spectra of *p*FT.[5] This would then fit with the appearance of the weak band at ~575 cm^{-1} being 28^{1}, both based on our previous work,[18] and the fact that it is common to see "component" vibrations of Δv = 0 vibtor and combination bands.

2. Band B

Band B in the REMPI spectrum is at 619.0 cm^{-1} which fits very well to the 30^{2} transition, with $2D_{30}$ being totally-symmetric. The 30^{1} transition was assigned in Ref. 5 and the present REMPI band is in the expected position for the overtone, as is one of the most intense ZEKE bands at 642 cm^{-1}, corresponding to the Δv = 0 transition. Interestingly, a ZEKE band at 698 cm^{-1} is also very intense, and this could be assignable as the symmetry-allowed 14^{2} transition. A band at this position was seen in ZEKE spectra that arose from a complicated REMPI feature in the region 395–420 cm^{-1} – which was discussed in depth in Ref. 5 – and is seen in other spectra discussed later in the present work; however, the much lower S_1 wavenumber for $2D_{14}$ (~398 cm^{-1}) would mean that it is not in the correct position to be excited directly and so would have to arise from Franck-Condon activity. This does not seem consistent with the observed large relative intensity of the 698 cm^{-1} ZEKE band and we work on the assumption that the latter is an additional Δv = 0 band, and so sought an alternative assignment.

First, we note that a weak ZEKE band at 428 cm^{-1} is observed, and this is 270 cm^{-1} lower than the 698 cm^{-1} band and so would correspond to the latter being a combination band involving the D_{19} vibration, and of overall a_1 or possibly b_2 symmetry (or G_{12} equivalents). There are two possible assignments of the 428 cm^{-1} ZEKE band: $20^{1}30^{1}$ and $19^{1}20^{1}m^{3(-)}$. Although $D_{20}D_{30}$ would be of overall a_2 symmetry, it would fit with the 698 cm^{-1} ZEKE band then being $19^{1}20^{1}30^{1}$, which is of overall b_2 symmetry and so HT-allowed. The observation of the $20^{1}30^{1}$ band would then be attributable to its being a component of the vibration with the main activity. However, the relative wavenumber of the $D_{19}D_{20}D_{30}$ S_1 transition is expected to be around 663 cm^{-1} and so does not fit in with the present excitation position to be the Δv = 0 band. We thus favour the alternative assignment of the 428 cm^{-1} band to the $19^{1}20^{1}m^{3(-)}$ transition and the 698 cm^{-1} band to $19^{2}20^{1}m^{3(-)}$, with the latter being totally symmetric in G_{12} and having an expected S_1 wavenumber of around

620 cm^{-1} (using values for D_{19} and $D_{20}m$=3(-) from our previous work)[5] – matching well the excitation position. The similar intensity of the 642 cm^{-1} and 698 cm^{-1} ZEKE bands is consistent with the S_1 band being two overlapped features corresponding to 30^2 and $19^220^1m^{3(-)}$.

Our favoured assignment for the 786 cm^{-1} ZEKE band is then $14^120^130^1$, based on the previously-determined position of the 14^120^1 and 30^1 (463 cm^{-1} and 321 cm^{-1}) ZEKE bands, respectively,[5] giving a composite value of 784 cm^{-1}, in excellent agreement with the observed band position. The observation of this ZEKE band could arise from further overlap in the S_1 state since the 14^120^1 and 30^1 transitions are coincident in the S_1 state,[5] and so it is not surprising that the 30^2 and $14^120^130^1$ transitions are also essentially coincident. We note that we might also expect to see a ZEKE band corresponding to the 14^220^2 transition, in this case the band should appear at about 926 cm^{-1}, and an extremely weak band can be seen at about 927 cm^{-1}, which may correspond to this transition.

Further on in the same ZEKE spectrum is a band at 797 cm^{-1}, which may be assigned as 17^120^1 based on a value for D_{17} in the cation of 685 cm^{-1}, which is consistent with other ZEKE bands discussed below. Taking this assignment, it is difficult to conclude that it arises from FC activity, and so we assume this is another Δv = 0 transition. The excitation position suggests a value for D_{17} in the S_1 state of 509 cm^{-1}; further discussion will be provided in Section IV.C.6.

In summary, we conclude that there is a remarkable coincidence in the position of a number of transitions that form Band B: 30^2, $14^120^130^1$, $19^220^1m^{3(-)}$ and 17^120^1, plus, very tentatively, 14^220^2.

3. Band C

The observed ZEKE features seen when exciting via Band C (625.0 cm^{-1}) suggest that the Δv = 0 ZEKE band(s) are significantly blue-shifted in relative transition wavenumber, compared to the REMPI one. (Although the wavenumber of REMPI Band C would be quite consistent with arising from the S_1 combination band, 11^120^2 (seen for *p*DFB)[3] there is no expected ZEKE band at 662 cm^{-1}.) The most likely assignment that has such a large shift upon ionization appears to be to the vibronically-allowed $D_{14}D_{18}$ vibration (overall b_2 symmetry); with the established value for D_{14}, this suggests a value for S_1 D_{18} of ~426 cm^{-1}. Although the latter is significantly below the calculated value, it is in line with the experimental versus calculated values for *p*DFB (see Table I); additionally, this value is consistent with that deduced from other ZEKE bands (see below). We note that with a value for D_{18} in the cation of 499 cm^{-1} (see below), we expect the 14^118^1 ZEKE band at 849

cm^{-1}, in excellent agreement with the observed ZEKE band with a maximum at 850 cm^{-1}. There appears to be a low-wavenumber shoulder (~840 cm^{-1}) to the latter ZEKE band, with the $14^1 19^1 20^2$ combination band being a likely assignment – this will have b_2 symmetry and is expected at ~843 cm^{-1}; however, the expected S_1 wavenumber for this band is 661 cm^{-1} and so it would not be excited directly. However, since these latter two levels are both of b_2 symmetry, it is possible that the $14^1 19^1 20^2$ and $14^1 18^1$ levels are in Fermi resonance in the cation. In such case, the 840 cm^{-1} and 850 cm^{-1} ZEKE bands would be better designated $14^1 19^1 20^2 \ldots 14^1 18^1$ and $14^1 18^1 \ldots 14^1 19^1 20^2$, respectively.

Our favoured assignment of the 651 cm^{-1} ZEKE band is to $28^1 m^4$, which is in about the correct position in the S_1 state and ties in with the observation of $28^1 m^{3(+)}$ for REMPI Band A – see above. Another possible assignment for this ZEKE band at 651 cm^{-1} would be the somewhat surprising $19^1 20^3 m^{3(+)}$. This is expected at 652 cm^{-1} in D_0^+ and 628 cm^{-1} in S_1, and so fits the REMPI and ZEKE band positions well. However, the appearance of a band for this vibration is hard to justify on Franck-Condon grounds; also, vibrational/torsional interactions with this band are likely to be weak owing to the significant difference in quantum numbers with any likely nearby band.

The above assignments suggest it is possible that there is at least one other $\Delta(v,m) = 0$ band, $28^1 m^4$, with an intermediate S_1 level degenerate with the $D_{14}D_{18}$ vibration, but the latter has the largest contribution at this excitation wavenumber.

4. Band E

Although the ZEKE spectra arising when exciting at position D (658.5 cm^{-1}) and via Band E (661.5 cm^{-1}) are very similar to each other, there are distinct differences. At position D, the ZEKE bands at ~715 and ~730 cm^{-1} appear relatively more intense. Exciting high rotational levels when exciting at position D could be the cause of broadening and double-peak structure of some of the ZEKE features seen, as many of these appear more cleanly via Band E.

The two most intense bands (at 684 cm^{-1} and 769 cm^{-1}) in the ZEKE spectrum recorded via Band E are of almost the same relative intensity, and so likely both $\Delta v = 0$ bands arising from essentially coincident S_1 levels. First, the ZEKE band at 769 cm^{-1} may be satisfactorily assigned to the totally-symmetric $18^1 19^1$ combination band, based upon both the experimental value for D_{19} in the cation, and also the observation of a weak ZEKE band seen at 499 cm^{-1} that may be assigned to the D_{18} vibration – one of the frequent

"component" ZEKE bands observed for $\Delta v = 0$ combination bands. The expected relative wavenumber for $18^1 19^1$ in the REMPI spectrum is ~668 cm^{-1} and so in line with the excitation position.

A possible assignment of the 684 cm^{-1} ZEKE band to $30^2 m^{3(+)}$ is precluded by the fact that the expected S_1 position for this is ~676 cm^{-1} – but particularly that the ZEKE band is too intense to be simply from FC activity, given the small intensity of the 30^2 transition (a contributor to Band B) A more plausible assignment for the 684 cm^{-1} ZEKE band is to $20^2 29^1 m^{3(+)}$, which is totally symmetric and although this has an expected S_1 wavenumber of ~675 cm^{-1}, and so shifted from the excitation position, there is good agreement with the cation value of ~686 cm^{-1} and the ZEKE band. This would suggest that overlap with the $18^1 19^1$ transition must occur (but with apparently very little interaction), and that therefore both the 684 cm^{-1} and the 769 cm^{-1} ZEKE bands are confirmed as $\Delta v = 0$ bands. The appearance of a ZEKE band at 718 cm^{-1} suggests activity from the D_{10} vibration, together with the weaker band at 732 cm^{-1}, whose assignment is uncertain, but is consistent with $17^1 m^{3(-)}$, either via FC activity, or perhaps by interaction in the cation, as the S_1 level is far from the excitation position – see discussion of Band G, below. We note that the calculated value for D_{10} suggests a value close to 700 cm^{-1} in the S_1 state, while deduced values for D_{18} and D_{19} suggest an S_1 value of ~668 cm^{-1} for the combination band; additionally, a value for $20^2 29^1 m^{3(+)}$ of 675 cm^{-1} may be deduced, based on previous values.[5] It therefore appears, as a result of various interactions, including with D_{10}, that the $D_{18}D_{19}$ and $2D_{20}+D_{29}m$=3(+) levels are essentially coincident at 662 cm^{-1} in S_1; it is possible, therefore that the D_{10} level may have been pushed up slightly in wavenumber.

The broadish ZEKE feature at 875–900 cm^{-1} may contain a contribution from 11^2 on the lower wavenumber side. A plausible assignment of the main part of the 890 cm^{-1} ZEKE feature is the vibtor transition, $16^1 m^{3(-)}$, which fits on symmetry grounds. Since it is difficult to see why this would be FC active, it would have to be a $\Delta(v,m) = 0$ transition (or possibly active in the $S_1 \leftarrow S_0$ transition via coupling and so then possibly in a slightly shifted position). The excitation position suggests an S_1 wavenumber of 621 cm^{-1} for D_{16}, which is consistent with the calculated versus experimental values for *p*DFB. A weak feature at 842 cm^{-1} can then be tentatively associated with 16^1.

In summary, Band E is concluded to arise from an overlap of three transitions, $18^1 19^1$, $20^2 29^1 m^{3(+)}$ and $16^1 m^{3(-)}$. Further, there is a possibility of interaction, mainly between $D_{18}D_{19}$ and D_{10}, which is discussed further in the following subsection.

5. Band G

The ZEKE spectra recorded at position F (706.5 cm^{-1}) and Band G (710.5 cm^{-1}) are very similar in the region of the Δv =0 transition (see Figure 2). One difference is the appearance of an apparent feature at 727 cm^{-1} when exciting at position F, and although this might be assigned as $20^{1}28^{1}m^{3(-)}$ it is more likely to be due to rotational profile effects.[5]

A longer ZEKE scan is shown in Figure 3 when exciting via Band G and we concentrate on this spectrum here. The clear Δv = 0 ZEKE band at 721 cm^{-1}, together with the S_1 band wavenumber of 711 cm^{-1}, strongly supports a major contribution from the D_{10} totally-symmetric vibration. As a consequence, we expect the majority of the more-intense bands in the ZEKE spectrum also to be totally-symmetric, but with weaker ones possibly assignable to vibronically-induced bands. Assignments of most of the bands in this spectrum are straightforward and are indicated in Figure 3 and so only key points are summarized here.

In addition to the Δv = 0 ZEKE band at 721 cm^{-1}, the two other close-lying bands to slightly higher wavenumber can be assigned as transitions to the totally-symmetric $D_{29}D_{30}$ (742 cm^{-1}) and $D_{18}D_{19}$ (770 cm^{-1}) combinations. (A possible assignment of the 770 cm^{-1} band to $10^{1}m^{3(+)}$ is excluded owing to the large relative intensity.) Since we see the $18^{1}19^{1}$ and 10^{1} bands here, but with the reversed intensities to when exciting via Band E, we conclude the corresponding vibrational levels are interacting in the S_1 state. Also, the S_1 $29^{1}30^{1}$ band is expected at 710 cm^{-1} in the S_1 state and so seems to be overlapped with the 10^{1} transition. The band assignable to $17^{1}m^{3(-)}$, observed when exciting via Band E, would also be expected here, if it arises from an interaction in the cation, and although there are indications of broadening on the blue edge of the main 10^{1} band, this is masked by the rise of the $29^{1}30^{1}$ band.

Owing to the good signal-to-noise for this spectrum, as well as the $18^{1}19^{1}$ ZEKE band at 770 cm^{-1}, we also observe weak features attributable to the 19^{1} transition and very weak bands, which can be attributed to the 11^{1}, $29^{1}m^{3(+)}$ and 18^{1} transitions, respectively. It is interesting to note that the D_{11} band is only observed extremely weakly from this fairly strong, totally-symmetric intermediate level, and also that D_{10} was not observed via D_{11}.[5] A weak shoulder (at 689 cm^{-1}) on the red edge of the main ZEKE band at 721 cm^{-1} can be assigned to the $20^{2}29^{1}m^{3(+)}$ transition. A broad feature at 319-360 cm^{-1} seems to contain two contributions, at 328 cm^{-1} and 353 cm^{-1}, possible assignments of these are to 20^{3} and 14^{1}. The lower-wavenumber, weak features support many of the higher-wavenumber assignments (see below), being the frequently-seen components of combination (or vibtor) bands.[5]

The overall appearance of the ZEKE feature at ~1550 cm^{-1} greatly resembles that of the cluster of features at ~720 cm^{-1} and the separation is consistent with the wavenumber of the D_9 vibration. Hence, we simply assign these higher wavenumber features as combinations of the 720–770 cm^{-1} ones with D_9. On the other hand, the ZEKE feature at ~1130–1230 cm^{-1} has a different overall appearance; notably, the most intense, first member of the feature is additional. However, the other features in the band do fit with being combinations with the D_{11} vibration, and so are assigned as such, as indicated in Figure 3. The first and most-intense band, at 1127 cm^{-1} within this feature may be assigned as $13^1 14^1$ on the basis of the established value[5] for D_{14} and the calculated value for D_{13}. Hence, working back, we can derive a value for D_{13} in the cation of 777 cm^{-1}, which is in very good agreement with the calculated value (Table I). Although the $13^1 14^1$ band could arise from FC activity ($D_{13}D_{14}$ is totally-symmetric), this would not explain its being locally the most intense ZEKE band in this region. Hence, we assume that it arises as a $\Delta v = 0$ band from an overlapped feature in S_1 at 711 cm^{-1}. This then suggests D_{13} in S_1 has a value of 512 cm^{-1}, which is in fair agreement with the calculated value. We note that the correspondence with the *p*DFB D_{13} vibrational wavenumber in the S_1 state is somewhat poor; however, that derived value of 588 cm^{-1} was tentative and not securely based on dispersed fluorescence spectra.[3] An alternative wavenumber for this vibration (Mulliken mode ν_9 therein– see Table I) discussed in Ref. 3 was 475 cm^{-1} and this is in much better correspondence with the value derived here for *p*FT, and we enter this value in Table I.

It is interesting to note, when comparing the 680–780 cm^{-1} regions of the ZEKE spectra obtained when exciting via Bands E and G, that the 770 cm^{-1} band is present in both cases, but is relatively more intense via Band E; also, the 721 cm^{-1} band is also present in both cases, but more intense via Band G. As indicated above, we interpret this in terms of Fermi resonance between the D_{10} and $D_{18}D_{19}$ vibrations in the S_1 state. We also note that although we see a strong 684 cm^{-1} ZEKE band via Band E, it has largely vanished when exciting via Band G. One explanation for the latter behaviour is that the assigned $2D_{20}+D_{29}m=3(+)$ level is not interacting significantly with the other two vibrations, owing to small anharmonic coupling caused by the larger difference in quantum numbers; on the other hand, there is only a difference of three quantum numbers between the D_{10} and the $D_{18}D_{19}$, and so that interaction is expected to be stronger. (We note that the 684 cm^{-1} band must be different to the weak band seen via Band I – see below – which is assigned as D_{17} there, since it is so intense via Band E and this would be unlikely for a b_1 symmetry vibration.)

In summary, Band G is dominated by 10^1, but D_{10} is concluded to be FR with $D_{18}D_{19}$, and so Bands E and G can be viewed as a FR pair. The expected coincidence of the $29^1 30^1$ transition with 10^1 complicates the issue, and it is possible that this is evidence of a further contribution.

6. Bands H and I

Exciting via the weak Band H at 718.5 cm^{-1}, located close to the blue edge of Band G gives a very different spectrum (see Figure 2). Again, it seems that there are either overlapping and/or interacting features here since there are three bands, at 952 cm^{-1}, 1034 cm^{-1} and 1052 cm^{-1}, of quite similar intensity. We also note that a 954 cm^{-1} band dominates the spectrum when exciting via Band I at 747.5 cm^{-1} and this suggests that it is the $\Delta v = 0$ band in the latter case. For the 954 cm^{-1} band to be the $\Delta v = 0$ band when exciting via Band I at 747.5 cm^{-1}, it must satisfy both the observed ZEKE band, and the REMPI band position; only an assignment to $17^1 19^1$ appears to satisfy these. Since the wavenumber for D_{19} has been established in both the S_1 and D_0^+ states,[5] the REMPI and ZEKE band positions allow us to establish the corresponding values for D_{17} as ~683 cm^{-1} in the cation. With the value of D_{17} in the S_1 state of 509 cm^{-1} derived in Section IV.C.2, this would suggest that the $17^1 19^1$ transition should appear at 751 cm^{-1}, and so the $D_{17}D_{19}$ level appears to have been pushed down in energy slightly in S_1. Both the $S_1$and D_0^+ values are in line with the experimental versus theoretical values for *p*DFB (Table I). Further, the assignment of the $17^1 19^1$ band when exciting via Band I is supported by the appearance of a weak ZEKE band at 685 cm^{-1}, which may be assigned as 17^1; additionally, a weak band at 1087 cm^{-1} may be assignable to $9^1 19^1$.

Although the 952 cm^{-1} ZEKE band, observed when exciting via Band H, could be the same as the one seen via Band I, there does not seem to be evidence for these two REMPI bands to arise from interacting levels, and so we conclude this is coincidental. In this case, an assignment to $16^1 20^1$ would fit with this being a separate $\Delta v = 0$ band. Since the wavenumber of D_{20} has been established in the S_1 and D_0^+ states, then the ZEKE and REMPI band positions lead to wavenumbers of D_{16} of 609 cm^{-1} and 841 cm^{-1}, respectively. In light of various interactions that may be occurring these values are in satisfactory agreement with those derived above from the tentatively assigned $16^1 m^{3(-)}$ ZEKE band, observed when exciting via Band E (Section IV.C.4). The alternative, as mentioned above, is there are interacting ZOSs in S_1 that give rise to Bands H and I; however, except for the appearance of the 952 and 954 cm^{-1} bands in both cases, no other band is common.

We now consider the other two bands in the ZEKE spectrum when exciting via Band H, at 1034 cm^{-1} and 1052 cm^{-1}. One plausible assignment for the 1034 cm^{-1} ZEKE band is to $14^1 17^1$, which is in the expected position based on the cation value for D_{17} just derived and the established value of D_{14}. There is no obvious reason why this band should be FC active, and so we assume this is a Δv=0 band. The excitation position suggests a value for D_{17} in the S_1 state of 520 cm^{-1}, but note that the assignments of the $17^1 20^1$ and $17^1 19^1$ bands above, together with their excitation positions, would suggest a slightly lower value. Even though there are no clear

bands assignable to b_2 symmetry vibrations near to Band H to perturb the $D_{14}D_{17}$ level, particularly to higher wavenumber, this seems the only viable assignment, and perhaps suggests a perturbation involving a Herzberg-Teller interaction.

Finally, the ZEKE band at 1052 cm^{-1}, seen when exciting via Band H, cannot be assigned to any obvious FC-active band, nor obvious Δv=0 vibrational combination band. We hence looked for possible vibtor transitions, identifying the most likely as being the FC-allowed $15^1m^{3(-)}$. This would suggest a value for D_{15} of 1008 cm^{-1} in the cation, and of ~678 cm^{-1} in the S_1 state, both in good agreement with the calculated values, with the latter value matching well the experimental versus calculated value for *p*DFB.

D. 750–811 cm^{-1}

There are no significant bands between 750 cm^{-1} and 790 cm^{-1} in this region of the REMPI spectrum, but we note that under some conditions, weak features to lower wavenumber arise from molecular complexes. For example, the two at 764 cm^{-1} and 770 cm^{-1} that arise from the *p*FT-Ar complex, and correspond to exciting the same vibrations in the complex as the 797 and 804 cm^{-1} bands of *p*FT. Conditions were optimized so that molecular complex bands were not of significant intensity compared to those of the bare *p*FT molecule. As a consequence, the first features of interest in this wavenumber range are the two prominent ones at 797 and 804 cm^{-1}, see Figures 1, 4 and 5, and it is possible that each of these arises from more than one contribution; in addition, there is another weaker REMPI feature to higher wavenumber, which will be addressed in the Section IV.E.

Because of the number of ZEKE spectra recorded across this region, we split the spectra into two groups each corresponding to one of the main REMPI features; these are presented as Figures 4 and 5 and in each case an expanded view of the relevant region of the REMPI spectrum is given as a vertical trace. In assigning the REMPI features, we first note that they are at a position that is approximately twice that of the bands located at 395-415 cm^{-1}, discussed in Ref. 5 and Ref. 6. The assignment of those was to eigenstates that were predominantly formed from the $2D_{14}$ overtone and the D_{11} fundamental ZOSs; these are of the same symmetry, but apparently interact only very weakly. The main lower wavenumber eigenstate is largely $2D_{14}$, while the main higher wavenumber one is largely D_{11}; in addition, the D_{29} vibration also contributed significantly to that region, but is of a different symmetry and so does not interact directly with the other two ZOSs.[5] We also observed two other weak features in the ZEKE spectrum when exciting via the 395-415 cm^{-1} features,[5] the first of which suggested there was a minor contribution from the D_{14} m = 6(-) vibtor level

to the eigenstates in this region. Additionally, a weak band was observed in the ZEKE spectrum and assigned to the $2D_{19}$ overtone; however, this band was concluded to arise from FC activity, since the 19^2 REMPI band was seen to higher wavenumber in that spectrum.

In addition, we note that the calculated wavenumbers (Table I) suggest that the D_9 a_1 fundamental is also expected in this region of the spectrum. The D_9 vibration is most closely associated with Wilson mode ν_1 and both the 797 cm^{-1} and 804 cm^{-1} bands were associated with this vibration by Okuyama et al.[16] In our previous work,[18] we assigned both of these main REMPI bands as a_1 fundamentals (ν_1 and ν_{12} in Wilson nomenclature). In passing, we note that although Wilson mode ν_1 can be associated with mode D_9 here, it is very difficult to identify Wilson mode ν_{12} since it loses its identity upon substitution (see Table I). There are also problems with the ν_{9b} label: as can also be seen from Table I, this vibration should be much higher in wavenumber (see Ref. 15 for comment on various switches and ambiguities in Wilson and Varsányi labels that have occurred in the literature, such as $\nu_{9b} \leftrightarrow \nu_{8b}$). Even taking the mode referred to as being ν_{8b}, it can be seen that this mode loses its identity somewhat upon substitution and so no single Wilson label is adequate.

In our earlier study,[18] we were unaware that Zhao and Parmenter[20] had earlier reassigned these bands to the 29^2 and 9^1 transitions (27^2 and 5^1 in Mulliken notation for a D_{2h} molecule – the notation used in that work), in that wavenumber order. Also apparently unaware of Ref. 20, Davies and Reid[21] concluded the involvement of the same overtone – denoted $2\nu_{9b}$ in Wilson/Varsányi notation in their work; the analysis of the observed quantum beating in this time-resolved study led the conclusion that both main bands arose from eigenstates that involved contributions from both D_9 and $2D_{29}$ – we shall comment on this work in Section V.B. For the region of the spectrum currently under discussion, we initially pursue assignments of the REMPI bands in terms of S_1 eigenstates composed of D_9 and the six combinations and overtones of the D_{11}, $2D_{14}$ and D_{29} ZOSs, with the possibility of small contributions involving D_{14} m = 6(-). As will be seen below, we shall concur with the significant involvement of the D_9 and $2D_{29}$ ZOSs.

From Table I, it can be seen that in the S_1 state we expect the D_9 vibration at ~ 805 cm^{-1} and we also expect overtones of the vibrations that give bands in the 395-415 cm^{-1} region at 796 cm^{-1} (14^4), 798 cm^{-1} (29^2) and 816 cm^{-1} (11^2), with approximate positions for the combinations at 797 cm^{-1} ($14^2 29^1$), 806 cm^{-1} ($11^1 14^2$) and 807 cm^{-1} ($11^1 29^1$). Bearing in mind that interactions between levels with the same symmetry may occur, and that the value for D_9 is an estimate based on calculations, then it is difficult to be sure about the energy ordering of the final eigenstates without evidence from the ZEKE spectra, presented below. Note that we

shall separate off the 11^2 transition, which will be seen to be somewhat separated from the others (see Section IV.E). To gain insight into the contributions of the other ZOSs, we note that these would give rise to ZEKE bands at approximately 1400 cm^{-1} (14^4), 832 cm^{-1} (29^2), 1116 cm^{-1} ($14^2 29^1$), 1140 cm^{-1} ($11^1 14^2$) and 856 cm^{-1} ($11^1 29^1$); the ZEKE band for D_9 is expected at ~ 811 cm^{-1} (Table I).

We first note that only extremely weak ZEKE bands could be observed that were even tentatively assignable to the vibtor levels $D_{14}D_{29}$ m=6(-) or $D_{11}D_{14}$ m = 6(-). This suggests that there are, at best, only very minor contributions from these ZOS levels to the eigenstates in this region – this is in agreement with the weakness of the $14^1 m^{6(-)}$ band in lower wavenumber region.[5] (We note that a third ZOS, $3D_{14}$ m = 6(-) would appear at around 1235 cm^{-1} in the ZEKE spectrum but this would be overlapped by the 6^1 ZEKE band.)

We now compare the first 1300 cm^{-1} of the ZEKE spectra recorded at the wavenumber of the centre of each of the two main REMPI bands, which are shown in Figure 6. It may be seen that there are stark differences in relative band intensities. These spectra are very similar to those reported in Ref. 18, although their assignment will be modified here. If we first concentrate on the 800-830 cm^{-1} region of the ZEKE spectrum, we can see that there are two main bands (824 cm^{-1} and 837 cm^{-1}), with both appearing relatively strongly when exciting through the centre of the lower wavenumber REMPI band (796.8 cm^{-1}). However, the spectrum is dominated by the higher wavenumber of the two ZEKE bands when exciting through the centre of the higher wavenumber REMPI band (803.6 cm^{-1}). This behaviour is essentially replicated by the two bands at 1260–1280 cm^{-1}, which are assigned as being combinations of the 824 cm^{-1} and 837 cm^{-1} bands with D_{11}. Given the expected wavenumbers for 9^1 and 29^2, it initially seems clear that these two ZEKE bands may be assigned as arising from the D_9 and $2D_{29}$ vibrations, respectively. The ordering of the two main REMPI bands is, however, not immediately obvious, since they are only 6.8 cm^{-1} apart and the wavenumber of D_9 is based on a calculated value, while that of $2D_{29}$ is based on doubling the fundamental wavenumber of 399 cm^{-1}. Further, as noted above, both these and other ZOSs in this region could interact and so the observed bands then arise from eigenstates whose make-up may involve several ZOSs.

We note that when exciting at 796.8 cm^{-1}, then we see bands assignable as 19^1, 14^1, 29^1 and 11^1, as we see for the origin,[5] and while most of these bands are also present when exciting at 803.6 cm^{-1}, the 19^1 band appears to be absent; additionally, the 14^2 band is more intense when exciting at 796.8 cm^{-1} (see Figure 6). Secondly, we note that new bands appear when exciting at 803.6 cm^{-1}, in particular the band at 1142 cm^{-1}. Although this could be assigned as $11^1 14^2$ (see below) this assignment does not tie in with the similar intensity of the 11^1 band in both ZEKE spectra (see Figure 6), nor the fact that the 14^2 band is more intense

when exciting at 796.8 cm^{-1}. A better assignment for the 1142 cm^{-1} band is to 28^2, based on the value for 28^1 established in ref. 18. Given that both the D_{28} and D_{29} vibrations have the same symmetry and similar motions,[15] then it seems to make sense that with the additional activity from 28^2, then the 803.6 cm^{-1} band should be assigned predominantly to 29^2, while the 796.8 cm^{-1} band should be assigned to predominantly 9^1. This also fits better with the expected value of ~832 cm^{-1} for $2D_{29}$ and the calculated for D_9, each in the cation. However, the strong beating pattern in Ref. 21 suggests that the S_1 eigenstates ought to be composed of significant mixtures of the D_9 and $2D_{29}$ ZOSs, while the ZEKE spectra, at first sight, appear to suggest that the second eigenstate is mainly composed of one ZOS, while the other is roughly an equal mix of the two – these points will be discussed further in Section V.B.

We now discuss the bands in the 1550 –1750 cm^{-1} region. At first sight, the appearance of the main bands here seems similar to that in the 800–850 cm^{-1} region, but as the expanded trace c in Figure 7 and comparison with traces a and b in Figure 7, shows, this is not the case. We note that this region of the ZEKE spectrum is at a wavenumber that approximately corresponds to the D_9 vibration above that of the two bands in the 820–840 cm^{-1} region, suggesting we should see bands attributable to 9^2 and 9^129^2 here, expected at approximately 1648 cm^{-1} and 1661 cm^{-1}. If the behaviour is the same as the other two regions shown in Figure 7, then we would expect a pair of bands to be seen when exciting at 796.8 cm^{-1}, and then largely a single intense band, when exciting at 803.6 cm^{-1}. The traces in Figure 7(c) show this not to be the observed behaviour. In passing, we note that the ZEKE band at 1582 cm^{-1} can be assigned as 11^128^2 and that it only appears when exciting at 803.6 cm^{-1}. It is the other bands on which we shall now focus here.

There are three bands that are seen when exciting via the origin, but their relative intensities then differ markedly when exciting via the 796.8 cm and 803.6 cm bands. Concentrating on these latter two spectra, first, the lower wavenumber band at 1634 cm^{-1} has a very similar intensity in the two traces, while the next two features (1648 cm^{-1} and 1659 cm^{-1}) each appear with appreciable intensity in only one of the two traces. It is thus clear that the behaviour here is not simply that of the 820–840 cm^{-1} bands in combination with a "spectator" D_9 vibration, as was the case for the D_{11} combination bands at 1260–1280 cm^{-1}. We first discuss the initial assignment of the bands. The band at 1648 cm^{-1} is clearly due to 9^2, that at 1659 cm^{-1} to 9^129^2 and that at 1678 cm^{-1} to 29^4. We assign the 1634 cm^{-1} band to 3^1, in agreement with the assignment in Ref. 18 (noting the different labelling used therein – see Table I). We can also identify very weak features at 1705 cm^{-1} and 1719 cm^{-1} that can be assigned to 9^111^2 and 11^229^2 (i.e. combinations of the D_{11} overtone with the two main bands at 820–840 cm^{-1}). We now discuss the intensities of the bands. First, the dominance of the 9^129^2 band when exciting at 803.6 cm^{-1} is in line with expectations based on both the 820–840 cm^{-1} and

1260-1280 cm^{-1} spectra; however, what is not expected is the almost complete absence of this band when exciting at 796.8 cm^{-1}, based upon the 820–840 cm^{-1} and 1260–1280 cm^{-1} regions – particularly when compared to the intensity of the 9^2 band. Also remarkable is the similarity of the 1634 cm^{-1} band in both spectra, especially given the different intensities of the other bands. We make some initial comments on these observations in the following, and discuss these points further in Section V.B.

That the 9^1 and 29^2 ZEKE bands appear with a similar intensity (Figure 6 and 7) when exciting at 796.8 cm^{-1} might suggest an intermediate eigenstate with largely equal mixtures of the two ZOSs; however, the dominance of the 29^2 band when exciting at 803.6 cm^{-1} apparently contradicts this. This observation, coupled with the apparently contradictory intensities of the bands in the 1550 –1750 cm^{-1} region, implies that when exciting via the lower eigenstate then there is a significant FCF for 9^2 as well as for 9^1; additionally, there is intensity in the origin band (concluded to arise from the D_9 ZOS[21]). Thus, the contribution of the D_9 ZOS to the lower eigenstate should be judged from the sum of the origin, 9^1 and 9^2 ZEKE bands (and possibly smaller amounts of higher overtones, not scanned here). Taken with the dominance of the 29^2 band when exciting via the higher-wavenumber eigenstate, this then might suggest that the two eigenstates are each dominated from a single ZOS in the S_1 state: D_9 for the lower state and $2D_{29}$ for the upper one. We note that this is only an apparent contradiction with the tr-SEVI data,[21] which concludes significant mixed character in the eigenstates – see Section V.B.

As well as the main bands just discussed, there are various others seen in the ZEKE spectra as we move through the REMPI features; these can be seen in the 2D-ZEKE spectrum presented in Figures 4 and 5. Since these ZEKE bands are relatively well separated in wavenumber from each other, their activity is indicative of contributions of various ZOSs to the S_1 eigenstates that contribute to the REMPI feature, which can be deduced by comparing the wavenumbers of the ZEKE bands with those given above. Interestingly, some of these are not observed as discrete contributions in our REMPI spectrum, suggesting that some bands are completely overlapped by the two main features; thus, as with the 2D-LIF approach,[36] the 2D-ZEKE spectra are a powerful tool for unravelling contributions to the spectra.

For example, when exciting at 794 cm^{-1}, i.e. on the red side of the D_9 REMPI band (trace a), we see two clear ZEKE bands at 1112 cm^{-1} and 1171 cm^{-1} (see Figure 4). The lower wavenumber ZEKE band can be assigned as a contribution from $14^2 29^1$ (b_2 symmetry) supported by the accompanying $11^1 14^2 29^1$ band at 1552 cm^{-1}. Initially, the assignment of the 1171 cm^{-1} ZEKE band seems straightforward as 7^1; however, it is unexpected that it appears prominently when exciting at this wavenumber, and quickly becomes relatively weaker as we

excite at higher wavenumbers, being largely absent when exciting at the band maximum, position c. This is particularly the case since D_7 is an a_1 fundamental and so it is strange that it does not appear prominently when exciting at the centre of the band that corresponds to an eigenstate dominated by another a_1 fundamental mode, D_9. In addition, D_7 in the S_1 state is far away from the point of excitation (expected at ~1120 cm^{-1} in S_1) and so its appearance would have to arise from FC activity, yet the other ZOS that is active here ($2D_{14}$+D_{29}) is of b_2 symmetry. Thus, this suggests that the 1171 cm^{-1} ZEKE band appears here by virtue of there being an S_1 level at ~ 794 cm^{-1} and that it is a $\Delta v = 0$ band. We thus sought an alternative assignment.

Although there are a number of possible assignments for this ZEKE band, few have the corresponding level in the S_1 state at the correct wavenumber. After much consideration, we eventually concluded that the FC-allowed $12^1m^{6(-)}$ vibtor transition was the mostly likely assignment, giving reasonable agreement with both the excitation position for its S_1 value, and the position of the ZEKE band. There is the possibility of interacting with D_9 in S_1, which is reasonable, given the low difference in the number of quanta, which would affect its precise position in S_1. This assignment would allow this ZEKE band to have a different behaviour with excitation position from the 1112 cm^{-1} band (since they are of different symmetry) as observed. With the assignment of the 1171 cm^{-1} ZEKE band to $12^1m^{6(-)}$, its appearance is by virtue of a significant contribution to the corresponding S_1 eigenstate appearing at this excitation position (which may have some contribution from the D_9 and $2D_{29}$ ZOSs). The persistence of this band, albeit weakly, when exciting across the region of the 796.8 cm^{-1} band could support a weak interaction between D_9 and D_{12} m = 6(-). This is supported by the fact that a wavenumber for D_{12} in the S_1 state of 616 cm^{-1} is derived below (see Section IV.E) and suggests that the D_{12} m = 6(-) band should be observed at ~800 cm^{-1}. This would be consistent with this level having been pushed down in energy slightly, for example by interacting with D_9. (It is also possible that the $12^1m^{6(-)}$ band is seen when exciting at 793.8 cm^{-1}, but then then 7^1 band is seen when exciting via the maxima of the two main REMPI bands.)

The other main ZEKE bands in this spectrum seem to arise from the low- and high-wavenumber rotational tails of the main 796.8 cm^{-1} band, i.e. from higher rotational levels of the D_9 level. This is confirmed by the broadening of the bands at 820-840 cm^{-1}, particularly noticeable when exciting via positions a and e. We note that no additional ZEKE bands are seen when exciting at positions d and e suggesting no additional underlying eigenstates contribute to the high wavenumber edge of the 796.8 cm^{-1} REMPI feature.

When exciting on the red edge of the $2D_{29}$ band (see Figure 5) at position f (800.6 cm^{-1}), we see a prominent ZEKE band at 1140 cm^{-1}, which can be attributed to 11^114^2. We note that a ZEKE band at 1142 cm^{-1} appears

when exciting through the centre of the band (trace h), which we assigned to 28^2 in the above. This band seems to be distinct from the 1140 cm^{-1} band, which has a different behaviour with excitation position. Indeed, looking carefully at expanded versions of spectra, we can see both the 1140 cm^{-1} and 1142 cm^{-1} bands when exciting at position f, with the latter appearing as a shoulder on the former.

Although the 1140 cm^{-1} ZEKE band appears strongly when exciting at 800.6 cm^{-1}, it only appears weakly when exciting at the other higher wavenumber positions. Similar behaviour is observed for a reasonably strong ZEKE band that appears at 1400 cm^{-1} when exciting at 800.6 cm^{-1}, which can be assigned to 14^4. It is notable that the D_{11} and $2D_{14}$ ZOSs were deduced to be only weakly coupled in the 395-415 cm^{-1} FR, with both being deduced to be bright.[5] Earlier, we noted that we would expect the 14^4 band at ~ 796 cm^{-1} and the 11^114^2 band at ~806 cm^{-1}. The appearance of the 1400 cm^{-1} ZEKE band thus suggests that the $4D_{14}$ ZOS is contributing at 800.6 cm^{-1} and we hypothesise that it has interacted with the D_9 ZOS and moved up slightly in wavenumber. The situation with the 11^114^2 band is less clear: although the 1140 cm^{-1} ZEKE band seems to be assignable to this transition, this would mean that the S_1 level has moved down significantly in wavenumber, which seems an unlikely scenario. It is now instructive to look at the ZEKE spectrum recorded when exciting at 810.8 cm^{-1} (trace k in Figure 5). Here we see that the 14^4 ZEKE band appears, together with a similarly-intense band corresponding to 14^2; however, there is no clear ZEKE band attributable to 11^114^2, although such a band could be contributing to the shoulder of a band at 1130 cm^{-1}. Further, this excitation position would be in about the correct position for the 11^114^2 band, particularly if it had moved up in wavenumber slightly. Thus, we tentatively conclude that the 14^2 band is a signature of the contribution of the 11^114^2 band to this region, but that the main $\Delta v = 0$ band is unexpectedly weak.

When exciting via Band j (807.4 cm^{-1}), we see the two most intense bands are at 856 cm^{-1} and 1299 cm^{-1}, which are straightforwardly assigned to transitions to b_2 modes $D_{11}D_{29}$ and $2D_{11}+D_{29}$, with 11^129^1 expected close to the excitation wavenumber in the S_1 state, and so the $\Delta v = 0$ band. There are also weak bands at 987 cm^{-1}, 1100 cm^{-1} and 1130 cm^{-1}.

The 1100 cm^{-1} band only appears when exciting via Band j, and hence is likely to be of b_2 symmetry; a possible assignment is to 12^120^1. The 987 cm^{-1} and 1130 cm^{-1} bands appear to increase in intensity when exciting via Band k; it thus seems these are of a_1 symmetry. The 987 cm^{-1} band can be assigned as 18^2 but also could be associated with 28^129^1; either of these would have to be FC active, with the 18^2 considered more likely owing to the assignment of a higher wavenumber REMPI band.[37] The 1130 cm^{-1} band is plausibly the FC-active 13^114^1 transition, seen when exciting via Band G, in line with the activity of the related 14^2 band.

Lastly the weak band at 1059 cm^{-1} seen when exciting via band k has a plausible assignment of $20^2 29^2$.

E. 811–821 cm^{-1}

We recorded ZEKE spectra at a number of positions across the feature in this range and show a portion of the REMPI spectrum and the various ZEKE spectra in Figure 8. In previous work,[18] we assigned the REMPI band to the D_{11} overtone. A Δv= 0 propensity argument would lead us to expect an intense ZEKE band at ~880 cm^{-1} and while a ZEKE band at about the correct position exists, it is not the most intense. This non-FC pattern of bands was noted in Ref. 18, covering the observed progression of bands: 11^1, 11^2 and 11^3. A discussion in that work, using Wilson[12]/Varsányi[13] notation, suggested that the ν_{6a} and ν_{7a} vibrations were coupled. (Although Table I suggests that there is no D_i vibration that can be associated with ν_{7a}, the wavenumber of the band associated with the latter suggests an assignment to D_5.) The explanation in Ref. 18 does not seem sound as phrased, however, since (to first order) interaction between normal modes does not occur per se, and is likely referring to Duschinsky mixing between these vibrations during the $D_0^+ \leftarrow S_1$ transition. Further consideration of the same spectrum, re-recorded in the present work (Figure 8), leads to a conclusion that this explanation is unlikely, owing to the strongest band being so much more intense than the Δv = 0 band. Since the Δv = 0 rule seems to work well when exciting via many other eigenstates, we therefore sought another explanation for the observations. We first note that the feature at ~ 1330 cm^{-1} is actually composed of pair of bands, as noted in Ref. 18 – see Figure 8. The lower wavenumber and less intense of these two, is at 1322 cm^{-1} – precisely where one would expect the 11^3 band to be, while the more intense component is at 1335 cm^{-1} – this is the band that was assigned as 5^1 ($7a^1$) in Ref. 18. Further, a double band appears at ~1770 cm^{-1}, which has a lower component at 1764 cm^{-1}, corresponding to 11^4 and the more intense one at 1774 cm^{-1} (D_{11} + 1335 cm^{-1}). Given its intensity, it seems likely that the 1335 cm^{-1} ZEKE band corresponds to a separate ZOS and, although it is very close to the wavenumber expected for the D_5 vibration, it is not clear why this would be so intense when exciting via $2D_{11}$ (and again would be highly contrary to the Δv = 0 propensity rule). Hence, another explanation was sought: that there is another vibration contributing to this region of the REMPI spectrum with gives rise to the 1335 cm^{-1} band as a Δv = 0 ZEKE band. This would have to be a vibration that shifted considerably between the S_1 state and the D_0^+ state and so be an overtone or combination band involving one or more vibrations of a_2 or b_1 symmetry. The only viable assignment appears to be the totally symmetric $12^1 14^1$ combination band, which requires D_{12} to have wavenumbers of 618 cm^{-1} and 985 cm^{-1} in the S_1 and D_0^+ state, respectively. These compare well with the respective calculated values of 588 cm^{-1} and 987 cm^{-1} – hence this is a reasonable assignment. We note that Knight and Kable assigned a reasonably strong band to $12^1 14^1$ ($7^1 8^1$ in their D_{2h} Mulliken labelling scheme), which seems to be an inherently bright band; thus, its observation here is not unexpected. The present

values for D_{12} are also consistent with the assignment of the 1171 cm^{-1} ZEKE band to $12^1m^{6(-)}$ when exciting at ~ 793.8 cm^{-1} – see Section IV.D. That the 12^114^1 level gives such a strong band in the ZEKE spectrum suggests it is likely a major contributor to this REMPI band.

It seems likely that various vibrational interactions will be present, and this is supported by the weak appearance of the 14^2 and various other weak bands in the 815-900 cm^{-1} region that are seen when exciting through the eigenstates dominated by D_9 and $2D_{29}$. That the 11^1 level is particularly, comparatively, strong in the ZEKE spectrum is intriguing and may arise as a sum of different FC contributions. We also note the gradual loss of structure/broadening that occurs when exciting via tranches of higher-*J* rotational levels, most apparent when exciting at positions corresponding to the wings of bands.

When exciting via a weak feature at 821 cm^{-1} just to the blue of the main feature a noisy spectrum results, but with a prominent ZEKE band at 908 cm^{-1}; this band does not appear in the other spectra presented in Figure 8 except perhaps weakly in trace p. At the present time, we are unable to put forward a sensible assignment of this band.

V. FURTHER DISCUSSION

A. Comparison with *p*DFB

Here we compare the assignments obtained above for the REMPI spectrum of *p*FT, with those of *p*DFB, including the fluorescence study of Knight and Kable.[3] As noted above, since the electronic excitation is a $\pi^* \leftarrow \pi$ excitation in both molecules, we would expect to see largely similar vibrational activity, since this should induce very similar geometry changes upon excitation. Indeed, our introduction of the D_i nomenclature[15] was to assist in ensuring the same vibrations are compared between molecules, so that this aspect can be commented on more meaningfully. In Table I we have presented the available values for both *p*FT and *p*DFB, also giving labels used in other work. It is immediately apparent that a mix of "Wilson" and "Varsányi" labels have been used, with a number of those labels differing between studies. Also, Mulliken labels are difficult to establish because of the ill-defined point-group symmetry of a molecule with a close-to-free rotor. We have included experimental values for *p*DFB mostly taken from Ref. 3, but with a reassignment of the S_1 D_{13} wavenumber. Although there is agreement for the three lowest wavenumber b_2 assignments, which are also in line with the corresponding values for *p*FT, the wavenumbers for several of the S_1 b_2 vibrations also look questionable, but we cannot comment further on this. In previous work on monohalobenzenes[38,39,40] and

para-disubstituted benzenes[1] we have note the lowest a_2 symmetry mode for the S_1 state seems to be difficult to describe using TD-B3LYP, and this is again apparent in Table I. Unpublished trial calculations by our group using the CIS approach show that this method also performs poorly, and so we do not concur with the conclusions of Ref. 31 that the CIS/6-31G* values presented therein for the S_1 state of *p*FT are reliable; similarly those for the S_1 state of *p*DFB in Ref. 41 seem similarly unreliable when compared to experimental values. Our present conclusions are, except for D_{14}, that the S_1 vibrational wavenumbers from TD-B3LYP calculations are more reliable than CIS or even CASSCF calculations. It would be expected, though, that higher-correlated methods would perform better, but at a significantly increased cost.

Unfortunately, we are unable to perform such a detailed comparison for the ZEKE spectra,[4] since many fewer spectra have been recorded; we have, however, previously made some comparison with the ZEKE spectrum recorded via the origin, in Ref. 1.

Figure 1 shows the assignments of the REMPI spectrum of *p*FT that have been discussed in the present paper with several of the lower wavenumber ones having been discussed in Ref. 5; the derived fundamental vibrational wavenumbers have been summarized in Table I. We also include the values summarized by Moss et al.,[42] some of which were estimated: it seems that many of the estimated values are in poor agreement with available values.

The assignments of the *p*DFB spectrum, discussed at various points in the present work, have largely been taken from the LIF study of Knight and Kable,[3] but we have changed the labelling to the D_i nomenclature of the present work, using the correspondences in Table I. In Ref. 3, we note that they used D_{2h} Mulliken labelling, but additionally they gave Wilson labels to the modes; Mulliken labels would obviously be different for *p*FT (and indeed difficult to construct). These Wilson modes often differ substantially from the Duschinsky breakdown given in Table I, and there is some variation in the assignment of Wilson[12]/Varsanyi[13] labels to various modes. However, once a consistent vibrational labelling scheme is used for both molecules then a large degree of similarity in the activity can be seen – Figures 1 and 9, see also below. (See also Ref. 1 for further comparison with the low-wavenumber region of the corresponding spectrum in *p*-xylene.)

We note that, excluding the torsional modes in *p*FT, the low wavenumber region has very similar activity, with the 20^2, 14^120^1, 14^2, 29^1 and 11^1 transitions seen – Figure 1. Interestingly, in *p*FT the 14^120^1 transition was almost perfectly coincident with the 30^1 transition, deduced from the activity in the ZEKE[5] (and DF[6]) spectra, while in *p*DFB only the 14^120^1 transition is observed. The 30^1 transition would be expected at around 350 cm^{-1} in *p*DFB but does not seem to be present in the LIF spectrum.[3] This is explainable in terms of symmetry, as the HT-allowed vibrations that correspond to the b_2 vibrations in *p*FT are only the b_{3g} ones: in *p*FT the D_{30} vibration is of b_2 symmetry and so HT-allowed, while in *p*DFB it is of b_{2u} symmetry and hence

vibronically forbidden. We also note that the 14^2, 29^1 and 11^1 vibrations are more separated in *p*DFB, and although the D_{29} and $2D_{14}$ vibrations are still close in wavenumber, they cannot interact as they are both fundamental normal modes, and of different symmetry; in *p*FT, the D_{29} and D_{11} bands are almost completely overlapped, as originally deduced in our earlier study.[18] Notably, the 11^1 band is relatively intense in *p*DFB, while it is much less so in *p*FT. This could be related to different extents of geometry change along the D_{11} vibrational coordinate, but also as discussed by Blease et al.[35] and ourselves in Ref. 1, could also be a result of HT activity arising from the involvement of a component of one of the excited states that gives rise to the vibronic activity in benzene; the energetic separation of the S_1 state and this excited state will determine the extent of induced vibronic activity. Although the latter is less discussed, it is the same as the mechanism that gives rise to the very well-known activity in b_2 vibrations in the $S_1 \leftarrow S_0$ transition, which indeed gives rise to the intensity of the 29^1 transition in both molecules. We note that it is not possible to compare the intensities of this particular transition in the two molecules directly, owing to the heavy overlap with the 14^2 transition in *p*FT. Slightly higher in wavenumber the 19^2 transition can be observed, and then 28^1 in both cases. The latter appears to be relatively more intense in the case of *p*FT. There then follow a series of weak features, many of which have not been assigned in the case of *p*DFB. One assignment that has been made was to 11^120^2, but here we concluded that a band in that position for *p*FT was actually due to 14^118^1 from the position of the $\Delta v = 0$ ZEKE band. In both cases a band due to 30^2 was observed, although this was only tentatively assigned in Ref. 3.

In the 730–830 cm^{-1} region of the *p*DFB spectrum are several bands with correspondences to those discussed above for *p*FT. The most intense band is the 9^1 band, but in contrast to *p*FT, the 29^2 band is much weaker, perhaps as it is further away in wavenumber, and so interacting less strongly, which would provide support for the D_9 being the ZOBS, with $2D_{29}$ being a ZODS. Also, the 11^2 band appears in the REMPI spectrum of *p*FT and we conclude some weak interaction with the other a_1 levels nearby. (There is some common activity in ZEKE spectrum for *p*FT recorded via $2D_{11}$, and those recorded via the eigenstates that are composed largely of D_9 and $2D_{29}$ – see further discussion below – but it is small.) However, owing to its closer proximity to the 9^1 transition, and on the basis of DF spectra, it was concluded in Ref. 3 that for *p*DFB the D_9 and $2D_{11}$ were clearly in Fermi resonance. Also seen as a prominent band in the *p*DFB spectrum is 12^114^1. As deduced above, this band is also seen here, but is overlapping the 11^2 band; it is unclear whether there is any significant interaction between them, but again interaction with nearby a_1 levels is indicated. This is a situation akin to that lower in wavenumber where the D_{30} and D_{14}+D_{20} levels are essentially degenerate, but do not appear to interact to any significant extent.[5] Also seen in *p*DFB are the 14^4 and 11^114^2 bands,[3] but it is notable that neither the 11^129^1 nor 14^229^1 bands are observed. In the present work, the indications are that the two main

features in the 790–830 cm^{-1} range in *p*FT are the two eigenstates made up of D_9 and $2D_{29}$ with contributions from 14^4, 11^114^2, 11^129^1 and 14^229^1 all being small.

In passing, we note that a band assigned to the 10^1 transition is clearly seen in *p*FT, but the corresponding band is absent in *p*DFB, which can be explained by symmetry: in *p*FT the D_{10} vibration is of a_1 symmetry, and so totally symmetric, while in *p*DFB it is of b_{1u} symmetry and so the fundamental is not symmetry-allowed. We shall now discuss the two eigenstates at ~800 cm^{-1} in *p*FT in more detail, referring to time-resolved studies.

B. Comparison with time-resolved studies

We shall first discuss the ZEKE spectra we recorded at the centre of the two main REMPI bands at ~ 800 cm^{-1}, which are shown in Figure 6, with expanded sections shown in Figure 7. We have already commented on these briefly in Section IV.D, and the conclusion was that exciting via the upper eigenstate yielded a ZEKE spectrum dominated by a band at 837 cm^{-1} in the $\Delta v = 0$ region, while exciting via the lower eigenstate yielded a ZEKE spectrum with two bands of approximately the same intensity, at 824 cm^{-1} and 837 cm^{-1}. Further consideration of the expanded views of the spectra in Figure 7 led to the conclusion that there were significant FCFs from the lower eigenstate to levels that differ from the 824 cm^{-1} $\Delta v = 0$ band by ±1 quantum. If we sum these contributions together, it suggests that the lower S_1 eigenstate also leads to predominant activity in a single mode in the cation – we shall come back to this shortly.

We now consider the time-resolved results. First, the most detailed discussion on time-resolved studies has come from the results of Davies and Reid,[21] who used a two-colour ionization scheme, as in the present work, but employing 1 ps width pulses. By exciting the molecules with one picosecond laser, and then ionizing the molecules with a second, it was possible to record slow-electron, velocity-map imaging (SEVI) photoelectron spectra after a controlled, variable delay. This allowed the time evolution of various photoelectron bands to be deduced when exciting a number of eigenstates coherently. In the present case, both the two main eigenstates at ~800 cm^{-1} were excited, and quantum beats were observed for several photoelectron bands. Although the resolution of the SEVI technique (~40 cm^{-1}) was significantly better than that used in an earlier study,[30] it still did not allow the resolution of the two $\Delta v = 0$ photoelectron bands at 820–840 cm^{-1}. With this in mind, for the detailed study of these two S_1 eigenstates, the origin photoelectron band was selected[21] on the grounds that one eigenstate gave a reasonably intense origin band, while the other did not (this conclusion arose from the observed time-dependent photoelectron spectra). There were two key deductions from that work. First, that a long quantum beat was observed, whose Fourier transform suggested that the main contribution arose from two eigenstates separated by 6.69 cm^{-1}; we note that we

determine a separation between the two REMPI bands in the present spectrum as 6.8 cm^{-1}, with the difference being well within the uncertainty of the two techniques. (A second, broader and much weaker peak in the Fourier transform was observed at 6.22 cm^{-1}, but its origin was less certain.) A second key observation was that the initial oscillating SEVI signal lost some intensity rapidly over the first ~30 ps, but then stayed at a constant value for over 500 ps. Further analysis and modelling of the time-dependent signal suggested that: (i) rotational incoherence effects were contributing to the observed quantum beating pattern; (ii) that the population of one of the cold torsional levels was lost rapidly, while the other remained; (iii) the eigenstates were made up from a close-to-equal mix of both the D_9 and $2D_{29}$ ZOSs; and (iv) it was likely that other undetermined ZOSs were present.

A first key discussion point is the third conclusion, since it apparently is in contrast to the indications of the ZEKE spectra recorded herein. To address this, we first make the following observation. In both the time-resolved SEVI study and the present ZEKE study, deductions on the nature of the intermediate S_1 level are made from the activity observed in the photoelectron spectrum. If the accessed cation levels of interest are "clean", that is they are not formed from interacting ZOSs (and that these closely resemble those in the S_1 state), then the photoelectron activity points to the S_1 state ZOS make-up, albeit with caveats covering differing FCFs and photoionization efficiencies. Thus, in our earlier study,[5] the D_{11} and $2D_{14}$ ZEKE bands were well separated and hence the ZOSs are not interacting, and hence their intensity could be related to the S_1 state ZOS make-up (and hence a conclusion that these levels were at most only very weakly interacting). In the present case, the two $\Delta v = 0$ ZEKE bands are only separated by ~11 cm^{-1} and so it is possible the associated states are made up from interacting ZOSs to some extent. We note, for example, that when exciting via the origin, see Figure 7(a), both the 9^1 and 29^2 ZEKE bands are seen, with the latter being about 25% as intense as the former. Although this could simply arise from FC activity, it could also arise as a result of interactions in the cation. If there are interactions between the D_9 and $2D_{29}$ levels in both the S_1 state and the cation, this could affect the observed photoelectron band intensities, and so conclusions therefrom. As a limiting case, if the interactions in the S_1 and cation states were identical, then we would expect diagonal FCFs to the $\Delta v = 0$ states, and hence only one ZEKE band to be seen when exciting from each S_1 eigenstate. Together with the possibility of the aforementioned differing FCF and photoionization efficiencies, the observed ZEKE intensities would then be consistent with the conclusions of the time-resolved study if there was significant coupling in the cation as well as the S_1 state.

Consistency is found when comparing to the time-dependence plot constructed from the intensities of the unresolved $\Delta v = 0$ band, shown in Ref. 43. The quantum beating observed shows that the integrated band intensity is changing with time. In addition, the intensity at $t = 0$ ps is lower than that at 2.5 ps, in line with

the lower eigenstate having a major contribution from D_9, the ZOBS (which has significant FC activity away from this unresolved feature), while the upper eigenstate has a major contribution from $2D_{29}$, the ZODS, (which has most of its intensity within the unresolved feature). This explains why there are oscillations of this integrated intensity, and why its variation is out of phase with that of the origin band, which mostly reflects the ZOBS alone.

The drop-off in intensity over the first 30 ps was interpreted[21] in terms of coupling to levels that were not covered by the picosecond pulse and/or had a weak oscillator strength, and seemed to be linked to one of the torsional levels. We are unable to say anything definitive about this latter point, as we are unable to resolve the different torsional contributions, but offer the following comments. From Table II, we see that the m = 0 levels are a_1' in G_{12}, while the m = 1 levels are e''. Considering a_1 vibrational levels, then dipole-moment allowed m = 0 vibtor levels can only couple to vibrational levels of a_1 C_{2v} symmetry; on the other hand, m = 1 vibtor levels of e'' symmetry can couple to a_1 and a_2 C_{2v} symmetry vibrational levels. Thus, in principle, there is the possibility for more interactions involving m = 1 vibtor states than m = 0 ones. Further, by definition, the m = 1 levels involve the methyl group internally rotating, and thus perhaps more likely to be interacting with vibrations.

We also note in passing that (see Figure 6) we see the origin when exciting via both of the main eigenstates at ~800 cm^{-1}. The relative intensities of these may be seen to be close to the derived ratio[21] of the square of the coefficients of the contributions of the D_9 ZOS to each of the two corresponding eigenstates, again providing further consistency between the conclusion of the two studies (under the assumption that the origin band only arises from D_9 and not $2D_{29}$,[21] and that there are minimal contributions from any other levels).

Finally, we note that when fluorescence from *p*DFB after exciting the 9^1 transition (see supplementary material associated with Ref. 3 and also DF spectra in Ref. 44) is monitored, then very little intensity is seen in the 9_1 transition, suggesting that there is a large change in geometry along that coordinate, consistent with progressions in this vibration, and D_{11}, which are common in the photoelectron spectra of substituted benzenes. Thus, the FCF explanation outlined above for *p*FT seems the most reasonable for the observed ZEKE behaviour.

VI. CONCLUSIONS

In this work we have presented a wealth of ZEKE spectra recorded when exciting through levels that appear in a 250 cm^{-1} region of the $S_1 \leftarrow S_0$ spectrum. What has been notable both in the present study, but also in Ref. 5 has been the number of overlapping transitions, and the extent of coupling, strong and weak, between

different ZOSs, including vibtor levels. Recording spectra at different excitation wavenumbers across features, has proven an extremely powerful tool. This, and identifying overlapping transitions, are greatly benefitted by significant changes in vibrational wavenumbers upon ionization, so the corresponding ZOS ZEKE bands are separate.

The lowest wavenumber region considered here contained some very weak features, but the worth of persevering with obtaining these spectra was shown in the various values of b_1 fundamentals that were obtained for the first time. The most intense (but still relatively weak) of these features was associated with the D_{10} vibration, which was also identified here for the first time. In addition, various transitions to vibtor levels were tentatively assigned.

We then investigated the two intense bands at ~800 cm^{-1}. Although these had been reported on by several workers, including ourselves, the assignment has varied. Through the recording of a series of ZEKE spectra at various positions through the main bands, we could follow the evolution of the activity and so assign the contributions to the REMPI band; even with so much data, there were some difficulties in obtaining a wholly clear picture. In Figure 9 we indicate the positions of the main contributions to the ~800 cm^{-1} REMPI feature and also show the correspondence with the same region for *p*DFB. It is of note that we see all six of the expected overtones and combinations to this spectral region for *p*FT, based on the assignments of the 395–415 cm^{-1} region[5] as well as the anticipated presence of the 9^1 transition. This shows the sensitivity of the ZEKE technique in picking out even quite weak contributions. An unexpected observation was the ZEKE band at 1171 cm^{-1}, which although this could have been assigned to the 7^1 transition, the intensity suggested it was more likely something else, and the $12^1m^{6(-)}$ transition was put forward. The high resolution of the ZEKE technique allowed us to identify the two main contributions in the $\Delta v = 0$ region for the two main REMPI bands, and then by examining the contributions to higher energy, we were able to provide some rationalization of the unexpected intensities of these. We then invoked some coupling between the $\Delta v = 0$ levels in the cation to explain the apparent anomaly between the conclusions of time-resolved studies and the present results. Taken together, there is further support for the assignment of the two main eigenstates in this region[21] being composed of ZOSs that resemble the cation D_9 and $2D_{29}$ vibrations, with majority contributions in that wavenumber order.

We note that in the 800–1000 cm^{-1} region of the ZEKE spectra shown in Figures 3, 4 and 5, there are a number of weak features that are in common. These suggest further weak couplings involving D_9 and $2D_{29}$ and in particular involving $2D_{11}$, $D_{12}D_{14}$ and other levels that contribute to a feature at 845 cm^{-1} in the REMPI spectrum, to be discussed in future work.[37]

Also of interest, to higher energy we were able to identify that a band previously assigned as 11^2 likely had a majority contribution from $12^1 14^1$, and so we were able to provide an alternative explanation to that previously offered[18] as to the anomalous intensities in the ZEKE spectrum via this level.

As noted in Section III, if the residual error in the calculation of the vibrational wavenumbers is similar for *p*FT and *p*DFB, then we would expect the ratio of the experimental to the theoretical value to be similar between the two molecules. Indeed, with the assignments of the b_1 and a_2 S_1 vibrational wavenumbers presented herein, we find this to be largely true and, albeit a weak test, this provides some further confirmation of the correctness of the assignments of these – mostly for the first time. As also indicated, we expect the calculated cation wavenumbers to be more reliable, and this is in general the case. In total, we have reported eight new or revised S_1 vibrational wavenumbers, and similarly for the cation.

By unravelling the results of the present study and rationalize them in the light of other results, we have been able to identify a large amount of consistency in the activity of *p*DFB and *p*FT in the $S_1 \leftarrow S_0$ transition. Further, comparison to the time-resolved studies led to the conclusion that is it of importance to be able to resolve all contributions to the spectrum to gain better insight into the observed behaviour. In particular, combining the results from both time-resolved photoelectron and high-resolution ZEKE spectroscopy is a powerful tool in unravelling the vibrational couplings in molecules.[45,46,47]

Lastly, we note that the usefulness of the idea of coupled states (vibrational, vibtor etc.) has its main use in comparison between molecules. For example, the local mode picture of vibrations is important in the identification of molecules via their spectra; consequently, the more delocalized the energy levels are, the less useful they are for this purpose. On the other hand, if the motion is dispersed over the whole molecule, then this allows more energy to be stored in a molecule without dissociation occurring to a large extent. There is also usefulness in chemical control experiments: if the coherent excitation of eigenstates leads to the clean production of a ZOBS at t = 0 that has a localized nature, then this can be used for selective photodissociation. Alternatively, if the ZOBS identity remains for long enough, perhaps an investigation of specific localized energy on chemical reactivity can be undertaken. Clearly, generally the more modes that become coupled the more delocalized the motions become, which is one of the key reasons for studying such details. What has been noticed by several workers is that despite the rapid rise in the density of states with even quite modest increases in molecular complexity, such as the introduction of a methyl group, the main couplings are between quite a small number of levels. Thus, it is the efficiency of coupling between levels that is also a main driver for the delocalization process, and this in turn leads to a rather sporadic occurrence of coupling at low energies; at high energies, however, this will become more and more common,

and the picture of a statistical distribution of energy will become prevalent. Relating this to the photostability of biomolecules as a function of their chemical structure is clearly an overarching theme of such studies.

Acknowledgements

We are grateful to the EPSRC for funding (grant EP/L021366/1). The EPSRC and the University of Nottingham are thanked for studentships to W.D.T. and L.E.W. We are grateful to the NSCCS for the provision of computer time under the auspices of the EPSRC, and to the High Performance Computer resource at the University of Nottingham. We are grateful for discussions with Warren Lawrance and Jason Gascooke (Flinders, Adelaide), Katharine Reid (Nottingham), and particularly Julia Davies (Leicester).

Table I: Calculated and experimental vibrational wavenumbers (cm^{-1}) for the S_1 and D_0^+ electronic states of *p*DFB and *p*FT

D_i	Mulliken ("C_{2v}")[a]	Mulliken (D_{2h})[b]	Wilson/Varsányi labels			S_1					D_0^+			
			Ref. 3[c]	Ref. 18[d]	Duschinsky[e]	*p*DFB		*p*FT			*p*DFB		*p*FT	
						B3LYP[f]	Expt[g]	Moss[h]	B3LYP[f]	Expt[i]	B3LYP[f]	Expt[j]	B3LYP[f]	Expt[i]
								a_1						
D_1	1	1(a_g)	2	2	**2**,7a	3143		(3071)	3130		3118		3116	
D_2	2	10(b_{1u})	20a	20a	**13**,20a	3131		(3071)	3105		3108		3101	
D_3	4	2(a_g)	8a	8a	**9a**	1519		(1723)	1528		1628		1628	1631
D_4	5	11(b_{1u})	19a	19a	**18a**,(20a)	1422	1335	1330	1432		1457		1454	
D_5	7	3(a_g)	7a	7a	1,7a,(2,6a)	1235	1251	1230	1213	1230	1350		1311	1332
D_6	8	12(b_{1u})	13	13	12,19a,20a,(13 18a)	1198	1015	1192	1185	1194	1274		1211	1230
D_7	9	4(a_g)	9a	9a	**8a**	1099	[1116]	(1128)	1120		1137		1158	1170
D_8	10	13(b_{1u})	18a	18a	**19a**,12	951	937	845	954		956		969	[k]
D_9	11	5(a_g)	1	1	**1**,6a,(7a,2)	820	818	795	805	797	823		811	824
D_{10}	12	14(b_{1u})	12	12	20a,12,(19a,13)	710	[666]	(672)	700	711	726		710	721
D_{11}	13	6(a_g)	6a	6a	**6a**,7a,(2,1)	414	410	410	410	408	435		437	440
								a_2						
D_{12}	14	7(a_u)	17a	17a	**17a**	501	583	584	588	618	972		987	985
D_{13}	15	9(b_{1g})	10a	10a	**10a**	429	475[l]	(560)	484	512	760	726	770	777
D_{14}	16	8(a_u)	16a	16a	**16a**	97	175	188	172	199	360	359	356	350
								b_1						
D_{15}	20	15(b_{2g})	5	5	**5**,10b	697	670	(650)	706	678	978		998	1008
D_{16}	21	28(b_{3u})	11	17b	**17b**,11,(16b)	667	619	(625)	651	607	864	859	832	842
D_{17}	22	16(b_{2g})	4	4	**4**,(10b)	567	528	539[m]	538	509	710		671	685
D_{18}	23	29(b_{3u})	16b	16b	**16b**,11,(17b)	487	438	438	468	426	506	508	488	499
D_{19}	24	17(b_{2g})	10b	10b	**10b**,(4,5)	279	274	241	243	242	289	303	266	271
D_{20}	25	30(b_{3u})	17b	11	16b,17b,11	124	120	110	110	110	123	127	109	111
								b_2						
D_{21}	26	18(b_{2u})	20b	7b	**20b**	3139		(3040)	3126		3117		3115	
D_{22}	27	23(b_{3g})	7b	20b	**7b**	3126		(3040)	3100		3109		3101	
D_{23}	29	24(b_{3g})	8b	8b	**9b**	1407	1516	(1707)	1427		1472		1383	
D_{24}	31	19(b_{2u})	19b	19b	**18b**,(19b,14,15)	1397		(1777)	1315		1388		1470	
D_{25}	32	20(b_{2u})	14	14	**15**,(14)	1317	1591	1584	935		1311		1301	
D_{26}	33	25(b_{3g})	9b	3	**3**,8b	1232	[933]	(1188)	1255		1238		1250	
D_{27}	34	21(b_{2u})	15	18b	**14**,19b	1022	1100	1114	1053		1096		1115	
D_{28}	36	26(b_{3g})	6b	6b	**6b**,(8b)	553	558	549	546	552	572		564	570
D_{29}	37	27(b_{3g})	3	9b	8b,6b,(3)	396	403	399	395	399	424	430	412	416
D_{30}	38	22(b_{2u})	18b	15	19b,14,(18b)	347	352	305	307	311	357		313	320

[a] Used in Refs. 18 and 29– these are rather misleading labels, as the numbering included the vibrations of the methyl group, which cannot be described in C_{2v}.

[b] D_{2h} labels using the usual Mulliken procedure.

[c] Given as Wilson labels in Ref. 3 without any detailed comment.

[d] Noted as being Wilson labels in Ref. 18, but seem actually to be Varsányi labels – these often are different between similar molecules, and the label, despite being those of Wilson, do not always match the actual motion of the vibration – see Refs. 14 and 15 for further discussion.

[e] These express the S_0 modes of *p*FT in terms of those of benzene, using a generalized Duschinsky approach involving artificial isotopologues – see text and Ref. 15. Values outside parentheses have mixing coefficients > 0.2 and are termed major contributions, with bolded values being dominant contributions (mixing coefficients > 0.5). Those inside parentheses are minor contributions, and have values between 0.05 and 0.2. If there is more than one contribution of each type, these are given in numerical order. Vibrations with a mixing coefficient < 0.05 are ignored.

[f] UB3LYP/aug-cc-pVTZ for cation and TD-B3LYP/aug-cc-pVTZ, each scaled by 0.97 – see text.

[g] Values taken from the fluorescence study of Ref. 3, which agree with our REMPI values. Note that values in square brackets are ones we think are dubious based on the poor agreement with the calculated value – these generally were not conformed by dispersed fluorescence in that work. We have taken the alternative value for D_{13} offered in Ref. 3 on the basis of its better agreement with the calculated value and other trends. See text for further comments.

[h] Values compiled in Ref. 42, values in parentheses were estimated therein. The labelling has been adjusted to that of the present work. Note that Varsányi labels are given therein, that mostly correspond to those given in Ref. 18. Some of these values supersede those from previous work. Note that in some cases, slightly different values may be obtained from different bands, owing to anharmonicity and other interactions. The REMPI values are likely reliable to 1 cm^{-1}, while the ZEKE values to 2–3 cm^{-1}.

[i] Values taken from this work, Ref. 5 and Ref. 18 – see text for details.

[j] Values taken from Ref. 4, with a change of labelling.

[k] Assignment in Ref. 18 now thought to be incorrect.

[l] Alternative value given in Ref. 3 is preferred – see text.

[m] Value given as 359 cm^{-1} in Ref. 42, we have assumed this was a typographical error and changed this to 539 cm^{-1} here.

Table II: Correspondence of the C_{2v} point group symmetry classes with those of the G_{12} molecular symmetry group. Also indicated are the symmetries of the different pure torsional levels.[a]

C_{2v}	G_{12}	m
a_1	a_1'	0, 6(+)
a_2	a_2'	6(-)
b_1	a_2''	3(-)
b_2	a_1''	3(+)
	e'	2,4
	e''	1,5

[a] Symmetries of vibtor levels can be obtained by combining the vibrational symmetry (in G_{12}) with those of the pure torsional level, using the D_{3h} point group direct product table. Vibrational symmetries are given in Table I.

Figure Captions

Figure 1: REMPI spectra of (a) *p*DFB and (b) *p*FT. The first 830 cm^{-1} are shown in each case, with the assignments discussed in the text. In the case of *p*FT, the indicated torsion/vibtor region has been discussed in depth in Ref. 5.

Figure 2: ZEKE spectra of *p*FT recorded via different intermediate levels in the 580–780 cm^{-1} range. The top trace shows the REMPI spectrum, with the letters indicating the excitation positions. The corresponding ZEKE spectra are then indicated in the subsequent traces. The indicated assignments are discussed in the text.

Figure 3: Longer ZEKE scan of *p*FT recorded via Band G, as indicated in Figure 2. Assignments are discussed in the text.

Figure 4: The top trace shows a section of the REMPI spectrum of *p*FT that was shown in Figure 1(b). The shaded area indicates the excitation region over which ZEKE spectra were recorded. The dashed lines link the excitation position with the corresponding ZEKE spectrum from the expanded vertical REMPI trace. The indicated assignments are discussed in the text.

Figure 5: The top trace shows a section of the REMPI spectrum of *p*FT that was shown in Figure 1(b). The shaded area indicates the excitation region over which ZEKE spectra were recorded. The ZEKE spectra were recorded using different excitation wavenumbers and the dashed lines link with the corresponding ZEKE spectrum from the expanded vertical REMPI trace. The indicated assignments are discussed in the text.

Figure 6: Comparison of the ZEKE spectra recorded in the centre of the two main REMPI bands at 796.8 cm^{-1} and 803.6 cm^{-1}; the traces are colour coded, as indicated. Both the correspondence in many of the bands, plus the contrast in their relative intensities can be seen. The assignments (see also Figures 4 and 5) are discussed in the text. The dashed line indicates the UV intensity over the spectral region scanned.

Figure 7: Indicated sections of the ZEKE spectra recorded when exciting via the origin and the two main bands at 796.8 cm^{-1} and 803.6 cm^{-1}: (a) the main bands at 810–850 cm^{-1}; (b) the region corresponding to the combinations of the main bands at 810–850 cm^{-1} with D_{11}; and (c) the region corresponding to the combinations of the main bands at 810–850 cm^{-1} with D_9. The spectra recorded via the 796.8 cm^{-1} and 803.6 cm^{-1} bands are on the same scales and were recorded using the same lasers and on the same day, under the same conditions. The spectra recorded via the origin were recorded on a different day, and the UV intensity was different for the ionization laser over the range scanned; hence, these have been scaled so that the intensity of the 9^1 band matched that of the spectrum when exciting via the 796.8 cm^{-1} band, and similarly for the $9^1 11^1$ and 9^2 bands in the other two regions. The relative intensities are discussed in the text.

Figure 8: The top trace shows a section of the REMPI spectrum of *p*FT that was shown in Figure 1(b). The shaded area is expanded on the right-hand vertical axis. The ZEKE spectra were recorded using different excitation wavenumbers and the dashed lines link the excitation position with the corresponding ZEKE spectrum. The indicated assignments are discussed in the text.

Figure 9: Summary of the major contributing ZOSs to the REMPI spectrum at different positions, as revealed by the ZEKE spectra: (a) *p*FT and (b) *p*DFB. These are expanded views of the same regions shown in Figure 1. See text for details of assignments.

Figure 1

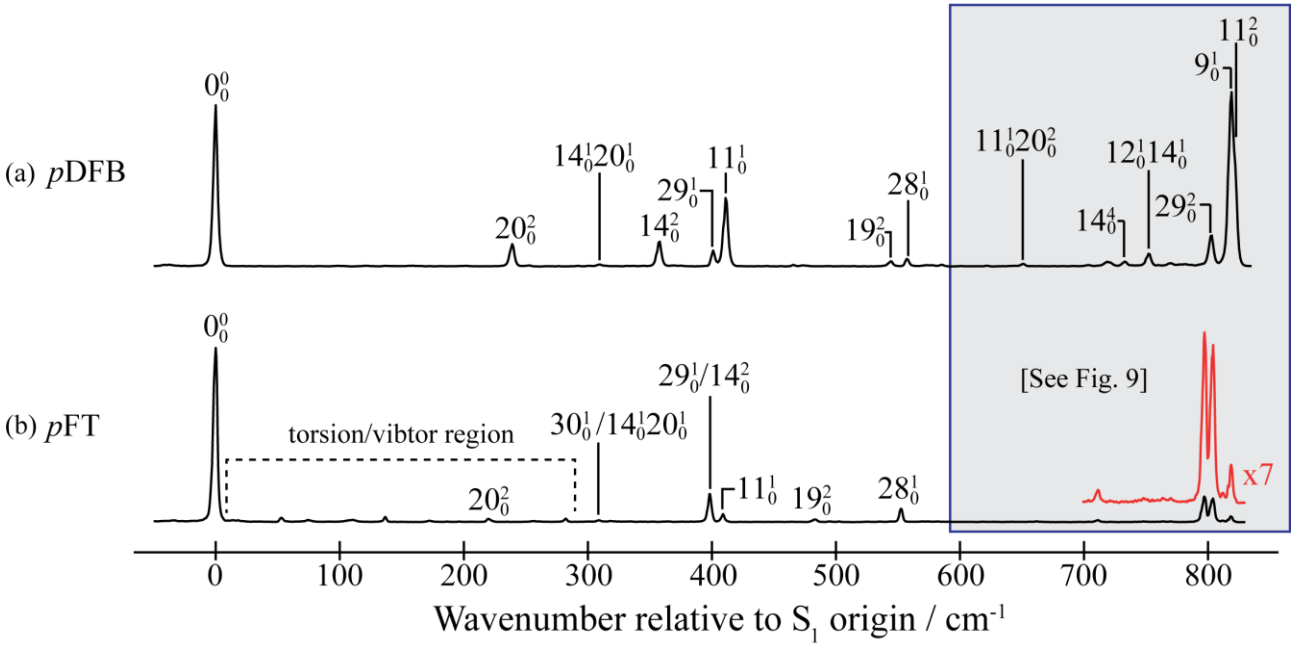
(a) pDFB
(b) pFT
torsion/vibtor region
[See Fig. 9]
x7
Wavenumber relative to S1 origin / cm-1
0
100
200
300
400
500
600
700
800

Figure 2

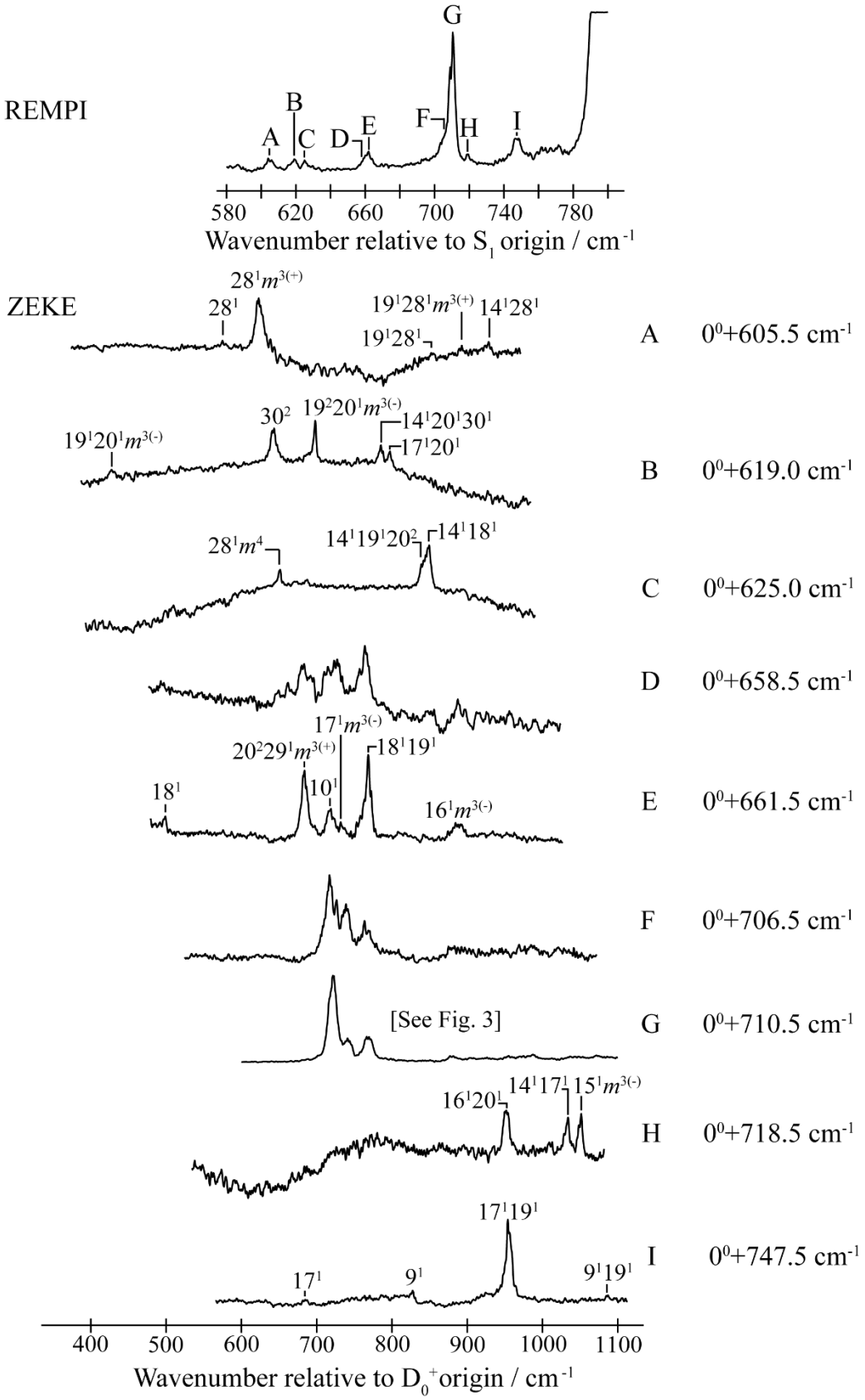
REMPI
A
B
C
D
E
F
G
H
I
580
620
660
700
740
780
Wavenumber relative to S1 origin / cm-1
ZEKE
28¹m³(+)
28¹
19¹28¹m³(+)
14¹28¹
19¹28¹
A 0⁰+605.5 cm-1
30²
19²20¹m³(-)
14¹20¹30¹
17¹20¹
19¹20¹m³(-)
B 0⁰+619.0 cm-1
28¹m⁴
14¹19¹20²
14¹18¹
C 0⁰+625.0 cm-1
D 0⁰+658.5 cm-1
17¹m³(-)
20²29¹m³(+)
18¹19¹
18¹
10¹
16¹m³(-)
E 0⁰+661.5 cm-1
F 0⁰+706.5 cm-1
[See Fig. 3]
G 0⁰+710.5 cm-1
16¹20¹
14¹17¹
15¹m³(-)
H 0⁰+718.5 cm-1
17¹19¹
17¹
9¹
9¹19¹
I 0⁰+747.5 cm-1
400
500
600
700
800
900
1000
1100
Wavenumber relative to D0+origin / cm-1

Figure 3

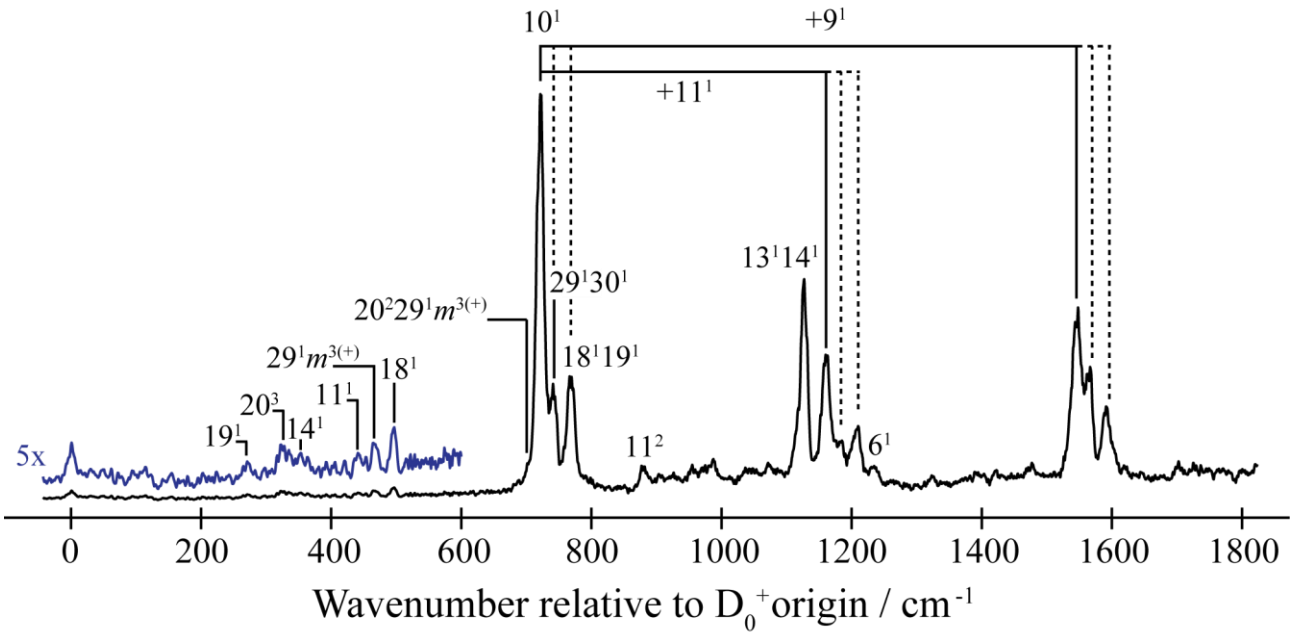
10¹
+9¹
+11¹
13¹14¹
29¹30¹
20²29¹m³(+)
18¹19¹
29¹m³(+)
18¹
11¹
20³
19¹
14¹
11²
6¹
5x
0
200
400
600
800
1000
1200
1400
1600
1800
Wavenumber relative to D0+origin / cm-1

Figure 4

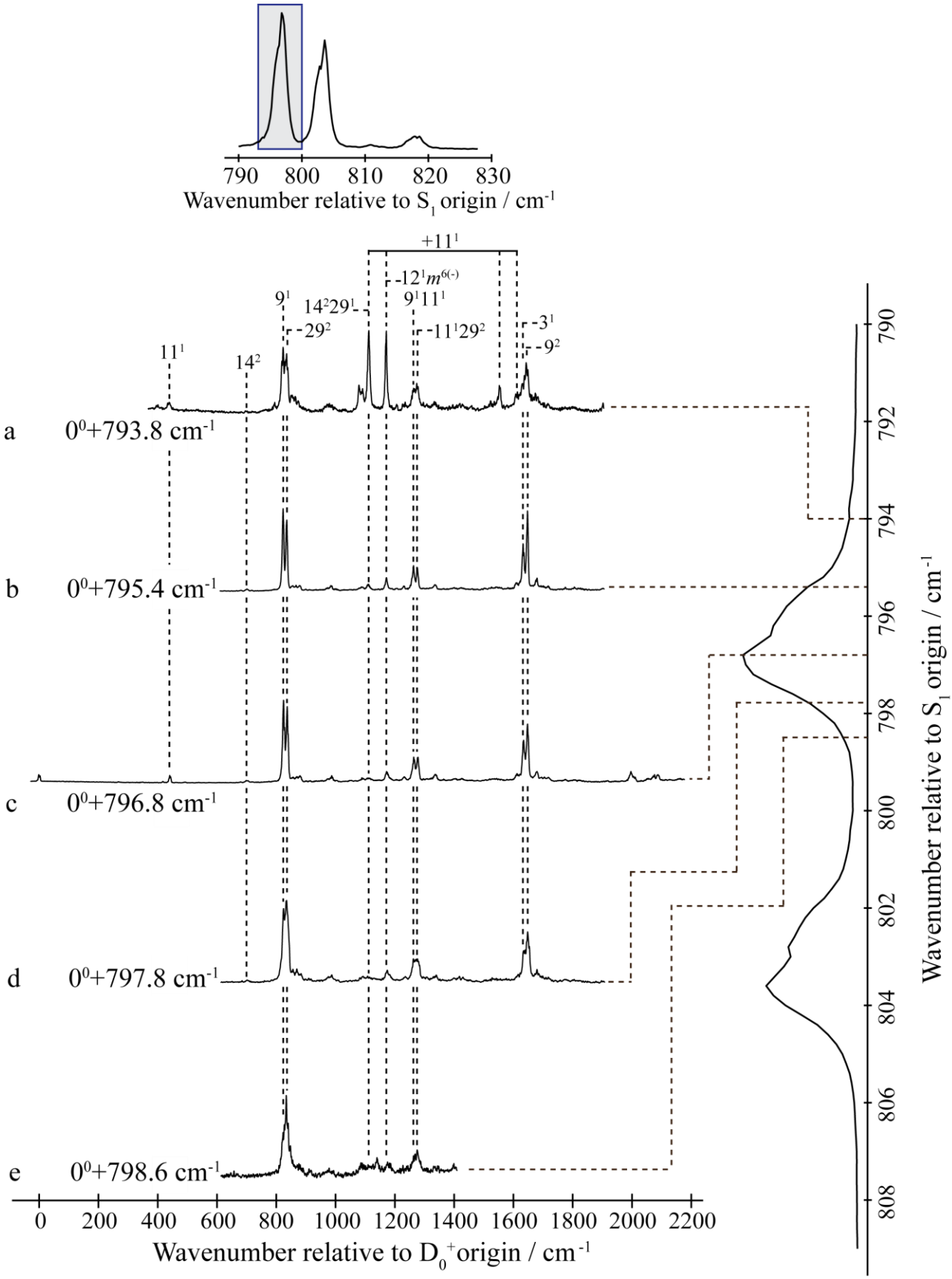
790 800 810 820 830
Wavenumber relative to S1 origin / cm-1
+11^1
-12^1m^6(-)
9^1
14^229^1
9^111^1
-29^2
-11^129^2
-3^1
-9^2
11^1
14^2
a 0^0+793.8 cm-1
b 0^0+795.4 cm-1
c 0^0+796.8 cm-1
d 0^0+797.8 cm-1
e 0^0+798.6 cm-1
0 200 400 600 800 1000 1200 1400 1600 1800 2000 2200
Wavenumber relative to D0+ origin / cm-1
790 792 794 796 798 800 802 804 806 808
Wavenumber relative to S1 origin / cm-1

Figure 5

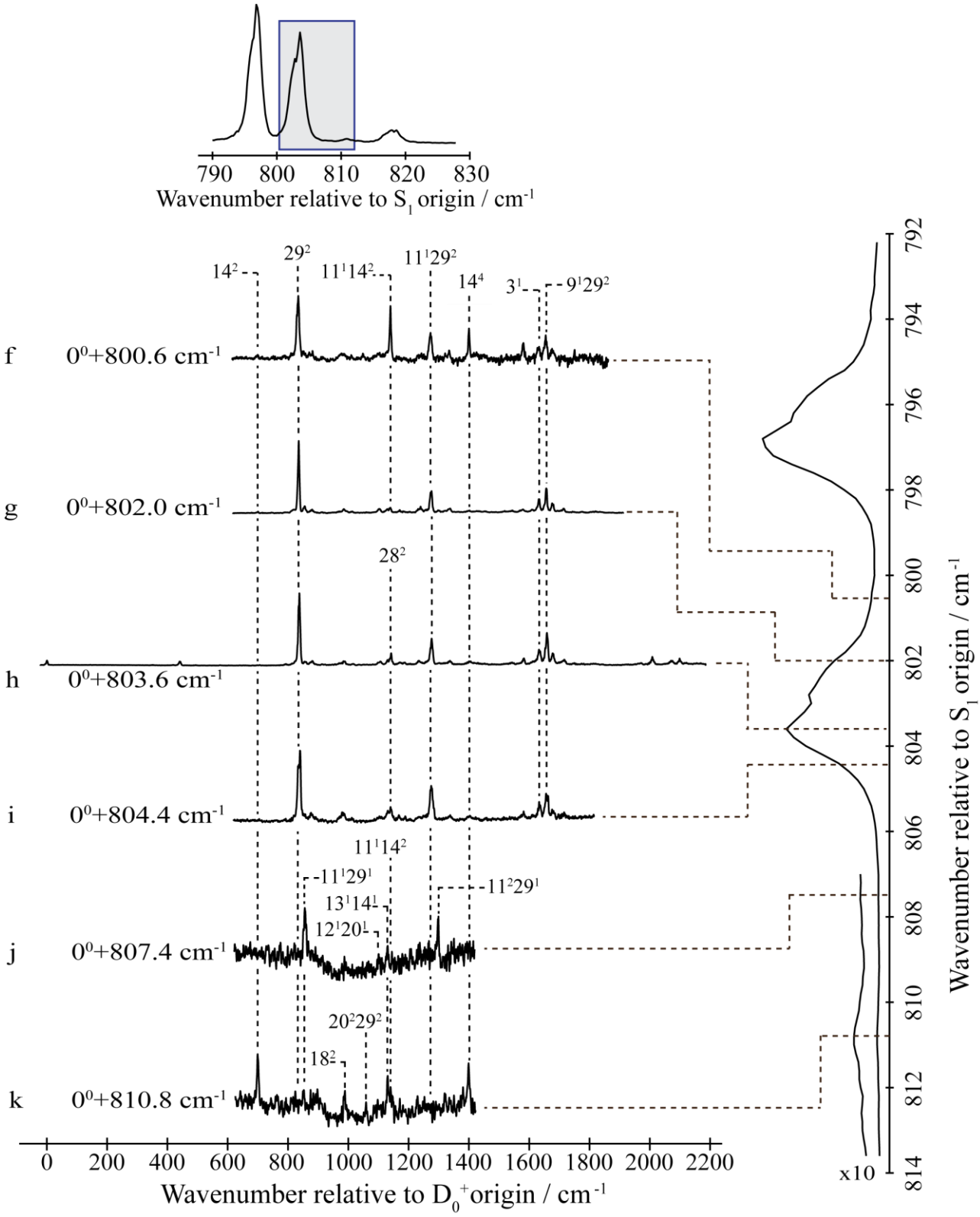
790 800 810 820 830
Wavenumber relative to S1 origin / cm-1
14²
29²
11¹14²
11¹29²
14⁴
3¹
9¹29²
f 0⁰+800.6 cm-1
g 0⁰+802.0 cm-1
28²
h 0⁰+803.6 cm-1
i 0⁰+804.4 cm-1
11¹14²
11¹29¹
13¹14¹
12¹20¹
11²29¹
j 0⁰+807.4 cm-1
20²29²
18²
k 0⁰+810.8 cm-1
0 200 400 600 800 1000 1200 1400 1600 1800 2000 2200
Wavenumber relative to D0+origin / cm-1
792 794 796 798 800 802 804 806 808 810 812 814
Wavenumber relative to S1 origin / cm-1
x10

Figure 6

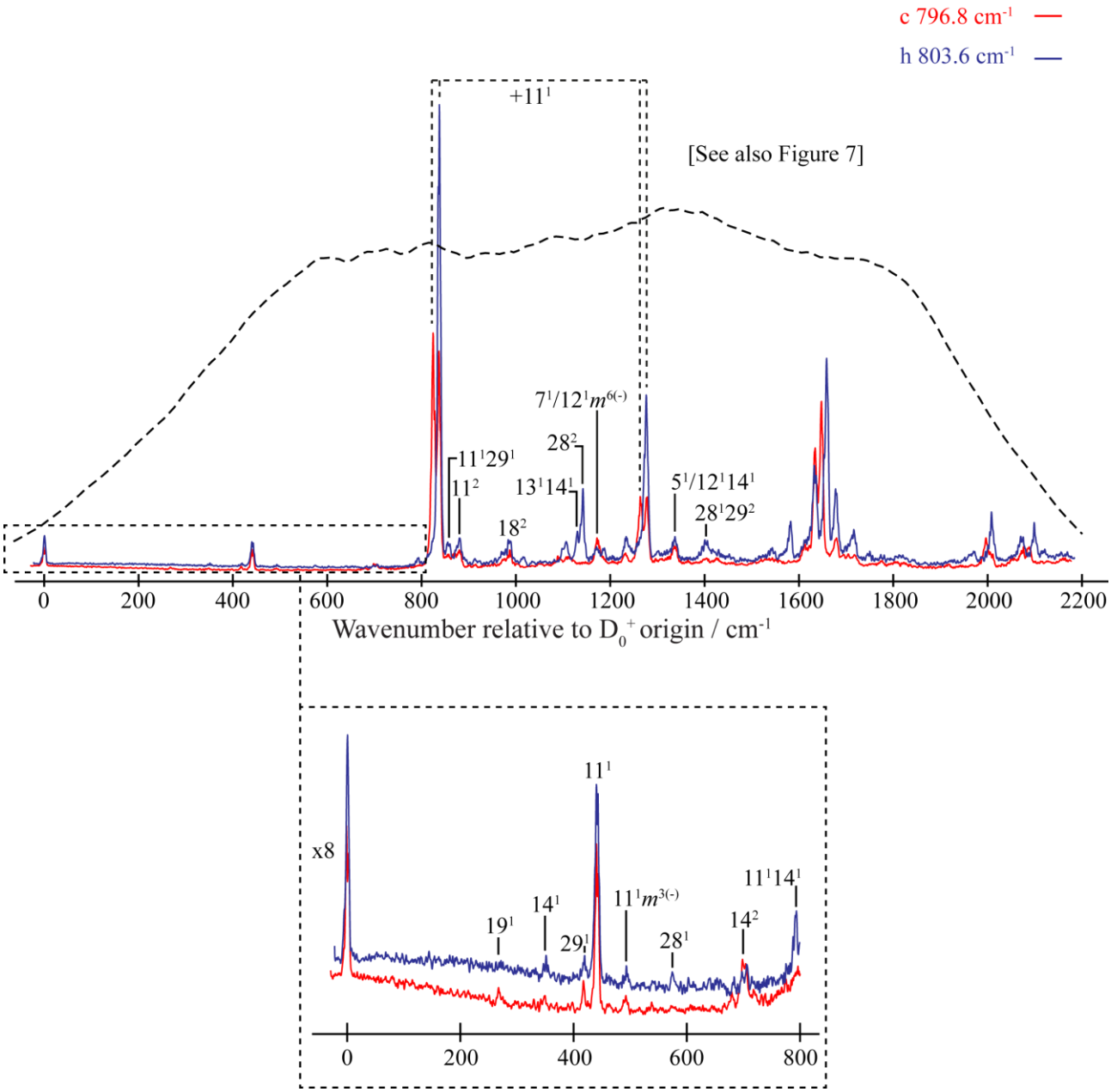
c 796.8 cm-1
h 803.6 cm-1
+11^1
[See also Figure 7]
7^1/12^1m^6(-)
28^2
11^129^1
11^2
13^114^1
18^2
5^1/12^114^1
28^129^2
0
200
400
600
800
1000
1200
1400
1600
1800
2000
2200
Wavenumber relative to D0+ origin / cm-1
x8
11^1
19^1
14^1
29^1
11^1m^3(-)
28^1
14^2
11^114^1
0
200
400
600
800

Figure 7

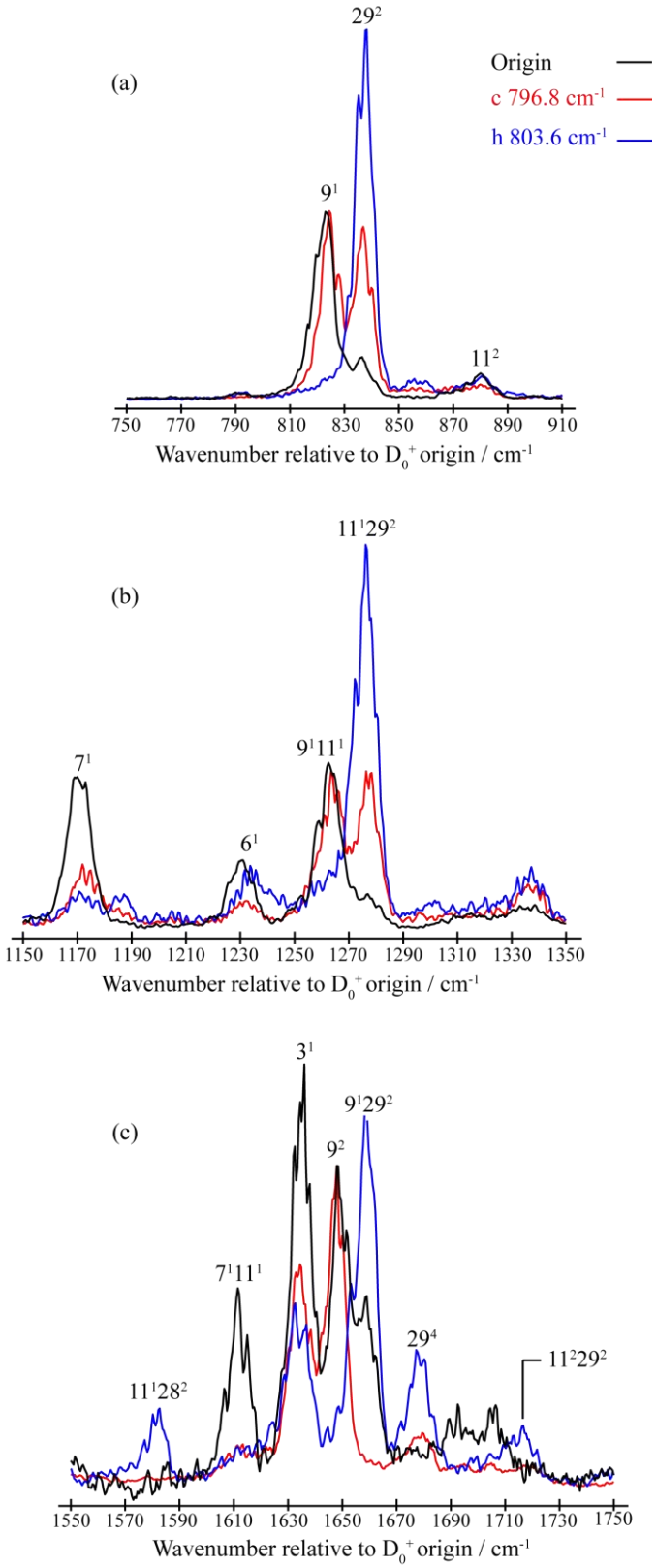
(a)
Origin
c 796.8 cm-1
h 803.6 cm-1
29²
9¹
11²
750 770 790 810 830 850 870 890 910
Wavenumber relative to D0+ origin / cm-1
(b)
11¹29²
9¹11¹
7¹
6¹
1150 1170 1190 1210 1230 1250 1270 1290 1310 1330 1350
Wavenumber relative to D0+ origin / cm-1
(c)
3¹
9¹29²
9²
7¹11¹
29⁴
11²29²
11¹28²
1550 1570 1590 1610 1630 1650 1670 1690 1710 1730 1750
Wavenumber relative to D0+ origin / cm-1

Figure 8

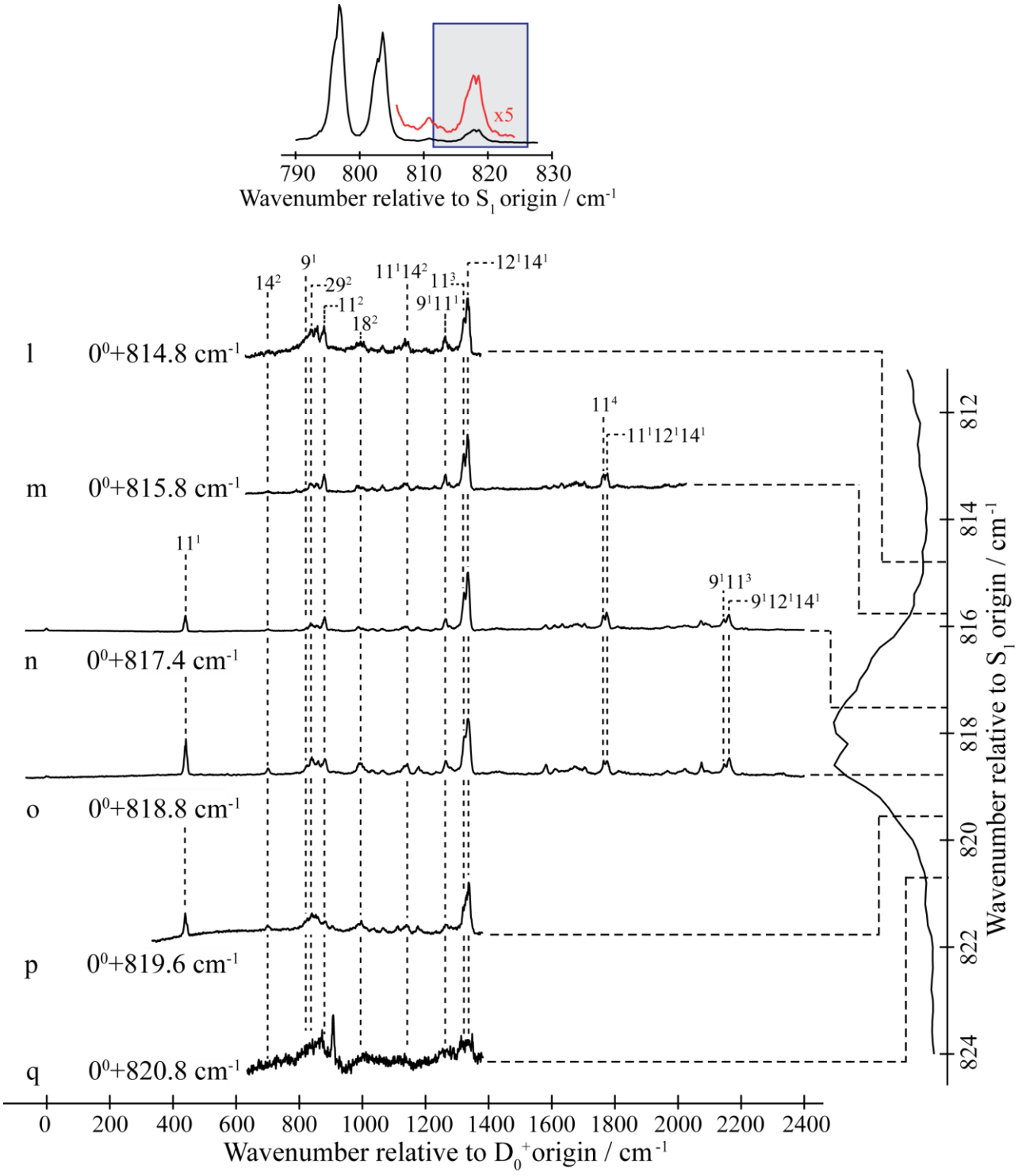
x5
790 800 810 820 830
Wavenumber relative to S1 origin / cm-1
14² 9¹ 29² 11² 18² 11¹14² 11³ 9¹11¹ 12¹14¹
l 0⁰+814.8 cm-1
11⁴ 11¹12¹14¹
m 0⁰+815.8 cm-1
11¹ 9¹11³ 9¹12¹14¹
n 0⁰+817.4 cm-1
o 0⁰+818.8 cm-1
p 0⁰+819.6 cm-1
q 0⁰+820.8 cm-1
0 200 400 600 800 1000 1200 1400 1600 1800 2000 2200 2400
Wavenumber relative to D0+origin / cm-1
812 814 816 818 820 822 824
Wavenumber relative to S1 origin / cm-1

Figure 9

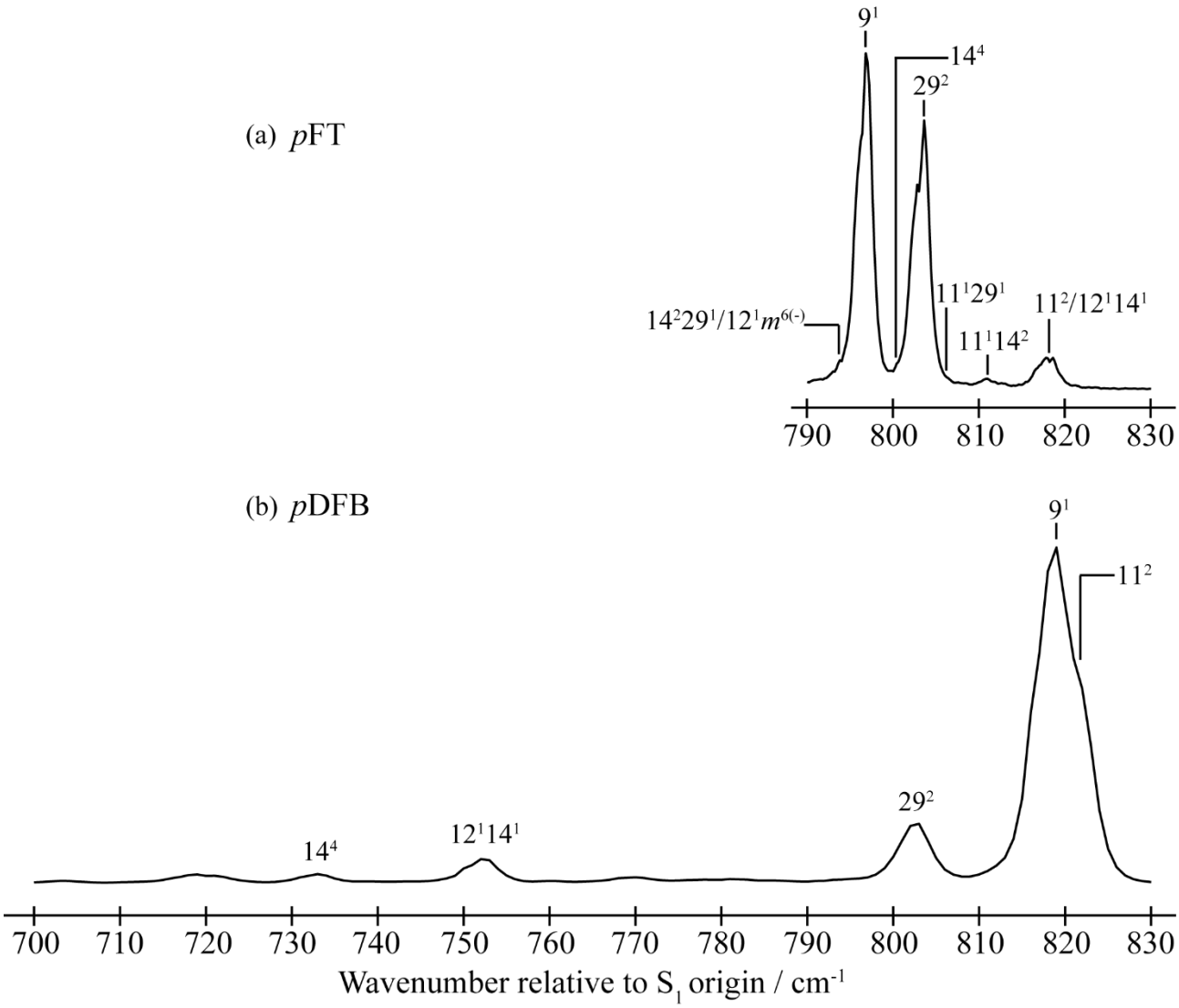
(a) pFT
9¹
14⁴
29²
11¹29¹
11²/12¹14¹
14²29¹/12¹m⁶(-)
11¹14²
790
800
810
820
830
(b) pDFB
9¹
11²
29²
14⁴
12¹14¹
700
710
720
730
740
750
760
770
780
790
800
810
820
830
Wavenumber relative to S1 origin / cm-1

References

[1] W. D. Tuttle, A. M Gardner, K. B. O'Regan, W. Malewicz, and T. G. Wright, J. Chem. Phys. **146**, 124309 (2017).

[2] A. M. Gardner, W. D. Tuttle, P. Groner, and T. G. Wright, J. Chem. Phys. **146**, 124308 (2017).

[3] A. E. W. Knight and S. H. Kable, J. Chem. Phys. **89**, 7139 (1988).

[4] G. Reiser, D. Rieger, T. G. Wright, K. Müller-Dethlefs, and E. W. Schlag, J. Phys. Chem. **97**, 4335 (1993).

[5] A. M Gardner, W. D. Tuttle, L. Whalley, A. Claydon, J. H. Carter, and T G. Wright, J. Chem. Phys. **145**, 124307 (2016).

[6] L. D. Stewart, J. R. Gascooke, P. G. Sibley, and W. D. Lawrance, "Methyl torsion, low-frequency vibrations and torsion-vibration states in S_0 and S_1 *p*-fluorotoluene" (unpublished).

[7] N. T. Whetton and W. D. Lawrance, J. Phys. Chem. **93**, 5377 (1989).

[8] R. A. Walker, E. Richard, K.-T. Lu, E. L. Sibert III, and J. C. Weisshaar, J. Chem. Phys. **102**, 8718 (1995).

[9] W. T. Cave and H. W. Thompson, Faraday Soc. Trans. **9**, 35 (1950).

[10] T. Cvitaš and J. M. Hollas, Molec. Phys. **20**, 645 (1971).

[11] C. J. Seliskar, M. A. Leugers, M. Heaven, and J. L. Hardwick, J. Molec. Spectrosc. **106**, 330 (1984).

[12] E. B. Wilson, Jr, Phys. Rev. 45 (1934) 706.

[13] G. Varsányi, *Assignments of the Vibrational Spectra of Seven Hundred Benzene Derivatives* (Wiley, New York, 1974).

[14] A. M. Gardner and T. G. Wright, J. Chem. Phys. **135**, 114305 (2011).

[15] A. Andrejeva, A. M. Gardner, W. D. Tuttle, and T. G. Wright, J. Molec. Spectrosc. **321**, 28 (2016).

[16] K. Okuyama, N. Mikami, and M. Ito, J. Phys. Chem. **89**, 5617 (1985).

[17] Z.-Q. Zhao, PhD Thesis, Indiana University (1992).

[18] V. L. Ayles, C. J. Hammond, D. E. Bergeron, O. J. Richards, and T. G. Wright, J. Chem. Phys. **126**, 244304 (2007).

[19] Z.-Q. Zhao, C. S. Parmenter, D. B. Moss, A. J. Bradley, A. E. W. Knight, and K. G. Owens, J. Chem. Phys. **96**, 6362 (1992).

[20] Z.-Q. Zhao and C. S. Parmenter, Ber. Bunsenges. Phys. Chem. **99**, 536 (1995).

[21] J. A. Davies and K. L. Reid, Phys. Rev. Lett. **109**, 193004 (2012).

[22] S. D. Gamblin, S. E. Daire, J. Lozeille, and T. G. Wright, *Chem. Phys. Lett.* 2000, **325**, 232.

[23] C. J. Hammond, V. L. Ayles, D. E. Bergeron, K. L. Reid, and T. G. Wright, *J. Chem. Phys.*, 2006, **125**, 124308.

[24] X. Zhang, J. M. Smith, and J. L. Knee, J. Chem. Phys. **97**, 2843 (1992).

[25] R. Seeger and J. A. Pople, J. Chem. Phys. **66**, 3045 (1977).

[26] R. Bauernschnitt and R. Ahlrichs, J. Chem. Phys. **104**, 9047 (1996).

[27] http://cccbdb.nist.gov/vibscalejust.asp

[28] Q. Ju, C. S. Parmenter, T. A. Stone, and Z.-Q. Zhao, Isr. J. Chem. **37**, 379 (1997).

[29] S. M. Bellm, P. T. Whiteside, and K. L. Reid, J. Phys. Chem. **107**, 7373 (2003).

[30] A. K. King, S. M. Bellm, C. J. Hammond, K. L. Reid, M. Towrie, and P. Matousek, Molec. Phys. **103**, 1821 (2005).

[31] J. A. Davies and K. L. Reid, J. Chem. Phys. **135**, 124305 (2011).

[32] R. S. Mulliken, J. Chem. Phys. **23**, 1997 (1955).

[33] G. Herzberg, Molecular Spectra and Molecular Structure II. Infrared and Raman Spectra of Polyatomic Molecules (Krieger, Malabar, 1991).

[34] E. Fermi, Z. Phys. **71**, 250 (1931).

[35] T. G. Blease, R. J. Donovan, P. R. R. Langridge-Smith, and T. R. Ridley, Laser Chem. **9**, 241 (1988).

[36] J. R. Gascooke and W. D. Lawrance, J. Chem. Phys. **138**, 134302 (2013).

[37] W. D. Tuttle, A. M. Gardner, L. E. Whalley, J. A. Davies, K. L. Reid and T. G. Wright, "Time- and frequency-resolved photoionization spectroscopy of coupled eigenstates of *p*-fluorotoluene". (unpublished)

[38] J. P. Harris, A. Andrejeva, W. D. Tuttle, I. Pugliesi, C. Schriever, and T. G. Wright, J. Chem. Phys. **141**, 244315 (2014).

[39] A. Andrejeva, W. D. Tuttle, J. P. Harris, and T. G. Wright, J. Chem. Phys. **143**, 104312 (2015).

[40] A. Andrejeva, W. D. Tuttle, J. P. Harris, and T. G. Wright, J. Chem. Phys. **143**, 244320 (2015).

[41] H. J. Elston, E. R. Davidson, F. G. Todd, and C. S. Parmenter, J. Phys. Chem. **97**, 5506 (1993).

[42] D. B. Moss, C. S. Parmenter, and G. E. Ewing, J. Chem. Phys. **86**, 51 (1986).

[43] J. A. Davies, L. E. Whalley, and K. L. Reid, Phys. Chem. Chem. Phys. **19**, 5051 (2017). Note that the $\Delta v = 0$ band referred to in the text here, is actually made up of two unresolved bands, corresponding to those observed in the present work – the figure caption to Figure 9 in that work is incorrect in that trace a is the integrated intensity of both of these unresolved bands (J. A. Davies, personal communication).

[44] K. W. Butz, D. L. Catlett, G. E. Ewing, D. Krajnovich, and C. S. Parementer, J. Phys. Chem. **90**, 3533 (1986).

[45] A. M. Gardner, A. M. Green, V M. Tamé-Reyes, V. H. K. Wilton and T. G. Wright J. Chem. Phys. **138**, 134303 (2013).

[46] A. M. Gardner, A. M. Green, V. M. Tamé-Reyes, K. L. Reid, J. A. Davies, V. H. K. Parkes and T. G. Wright J. Chem. Phys. **140**, 114038 (2014).

[47] J. A. Davies, A. M. Green, A. M. Gardner, C. D. Withers, T. G. Wright and K. L. Reid Phys. Chem. Chem. Phys. **16,** 430 (2014).